Groundwater for Sustainable Development 23 (2023) 100992

Contents lists available at ScienceDirect

Groundwater for Sustainable Development

journal homepage: www.elsevier.com/locate/gsd

Research paper

Effects of the 2021 La Palma volcanic eruption on groundwater resources (part II): Hydrochemical impacts

Alejandro García-Gil [a,*], Jon Jimenez [b], Samanta Gasco Cavero [a], Miguel Ángel Marazuela [a], Carlos Baquedano [a], Jorge Martínez-León [a], Noelia Cruz-Pérez [c], Chrysi Laspidou [d], Juan C. Santamarta [c]

[a] Geological and Mining Institute of Spain (IGME), Spanish National Research Council (CSIC), C/ Ríos Rosas 23, 28003 Madrid. Spain
[b] Dept. of Earth Sciences, University of Zaragoza, Pedro Cerbuna, 12, 50009 Zaragoza, Spain
[c] Departamento de Ingeniería Agraria y Del Medio Natural. Universidad de La Laguna (ULL), La Laguna (Tenerife). C/ Pedro Herrera, S/n, 38200, San Cristóbal de La Laguna. Spain
[d] Department of Civil Engineering, University of Thessaly, Volos, Greece

HIGHLIGHTS

- Tajogaite volcano eruption: Hydrochemical changes & impacts on groundwater.
- Significant trace element variations during volcanic eruptions revealed.
- Groundwater resilience demonstrated in the face of volcanic hazards.
- Importance of frequent monitoring for sustainable water management.
- Unveiling interactions between volcanic eruptions and groundwater quality.

GRAPHICAL ABSTRACT

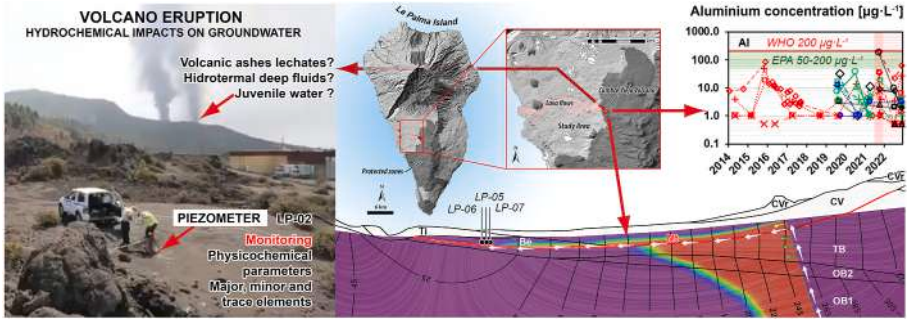

ARTICLE INFO

Keywords:
Volcanic eruption
Groundwater resources
Groundwater quality
Tajogaite volcano
Volcanic aquifers
La palma island
Canary islands

ABSTRACT

Volcanic eruptions can have significant implications for the management and sustainability of water resources in volcanic islands. The recent 2021 eruption of the Tajogaite volcano in La Palma Island (Canary Islands, Spain) raised concerns regarding its potential impact on groundwater resources. This study is the second part of a series investigating the hydrogeochemical impacts of the eruption. The study involved conducting three groundwater sampling campaigns during the eruption and two after the eruption, six months and one year after the eruption ceased. A total of 15 monitored points, including piezometers, wells, water galleries, and main gully collector of the island, all relatively close (2–15 km) to the erupted volcano, were sampled for the analysis of major, minor, and trace elements, physiochemical parameters, which were measured on-site. Statistical analyses were performed to assess the differences in groundwater composition before, during, and after the eruption. To evaluate the differences in water quality compared to pre-eruption events, 33 additional historical groundwater samples provided by the local Water Authority were assessed, and 103 groundwater analysis results from the groundwater data base of the Spanish National Geological Survey (IGME) were considered. The results of the study

* Corresponding author.
E-mail addresses: a.garcia@igme.es (A. García-Gil), jimenezbjon@posta.unizar.es (J. Jimenez), ncruzper@ull.edu.es (N. Cruz-Pérez), laspidou@uth.gr (C. Laspidou), jcsanta@ull.es (J.C. Santamarta).

https://doi.org/10.1016/j.gsd.2023.100992
Received 18 June 2023; Received in revised form 14 July 2023; Accepted 18 July 2023
Available online 1 August 2023

showed low but statistically significant changes in pH, T, conductivity and groundwater composition, mainly related to the high increases in several trace element concentrations, such as Al, Cr, Fe, Mo, Ni, Sr, Th, Tl, V, Zn, Ba, Cd, Co, Cu, Pb and U, with increments in various orders of magnitude for several elements. This increase was found to be highly influenced by the sample distance to the volcano during the eruption stage. The significance of these findings lies in their usefulness to enhance our understanding of the effects of volcanic eruptions on groundwater quality resources and demonstrate their resilience to this hazardous phenomenon, which ultimately underscores their reliability.

1. Introduction

Volcanic islands are often characterized by their isolation, fragility, and dependence on the availability of water resources (Kim et al., 2020; Kolomyts, 2019; Santamarta et al., 2014). The hydrogeology of volcanic aquifers is a critical component of these systems, providing water for drinking, agriculture, and other economic activities (Custodio et al., 2016; Duncan, 2012; White and Falkland, 2010). Due to their isolation, limited capacity for storage, and irreplaceable nature, freshwater aquifers found on oceanic volcanic islands are susceptible to contamination from anthropogenic sources and the intrusion of seawater (García-Gil et al., 2022; Gasco-Cavero et al., 2023; Mair and El-Kadi, 2013; Tribble, 2008). Furthermore, volcanic eruptions in these volcanic islands can strongly affect the island's hydrology (Herd et al., 2005; López-Saavedra and Martí, 2023), ultimately leading to potential biological and health hazards due to water and food supply contamination and worsening of hygienic conditions (Aubaud et al., 2013; Wiemken et al., 1981). The interplay between hydrothermal and hydrological processes at restless volcanoes is so intricate and influential that monitoring the associated activity is a fundamental tool for detecting and predicting volcanic unrest (Jasim et al., 2019). Valuable insights into volcanic activity can be obtained by monitoring variations in the chemical composition and temperature of groundwater, surface water, and steam at a volcano (Barberi et al., 1992). Furthermore, chemical anomalies in water composition have been recognized as identifiable precursors of subsequent volcanic activities (e.g. Carapezza et al., 2004), including phreatic explosions (Armienta and De la Cruz-Reyna, 1995).

There are two primary ways in which volcanic eruptions can impact the quality of freshwater resources in volcanic islands. The first one is through the mixing of surface water and/or groundwater with volcanic ash-leachates, which are generated from volatile substances deposited by volcanic plumes and adsorbed onto the surface of non-weathered ash (Witham et al., 2005). The deposition of volcanic ash with adsorbed volatiles contributes to the rapid delivery of elements and ions to the ground, with leaching occurring upon contact with rainfall or surface water flow (Delmelle et al., 2000). In these cases, an increase in the concentrations of Fe, F, As, SO_4 and Cl, as well as in the acidity and turbidity, have been reported as a consequence of the volcanic ash fall contaminating the water supplies (Auge et al., 2013; García et al., 2012; Kruse and Ainchil, 2003; Nicolli et al., 1989; Smedley et al., 2002). Alternative research has associated the heightened concentration of trace elements with the phenomenon of desorption from Al/Fe/Mn oxides (Bhattacharya et al., 2006; Gomez et al., 2009; Smedley and Kinniburgh, 2002). One of the main concerns regarding this affection is the fact that, due to the input of volcanic ash into the water supply, F concentrations have increased in certain cases exceeding the safe limits for human and animal consumption and reaching concentrations close to 10 mg/L (Stefánsson et al., 1957; Cronin et al., 2003). Variations in leachate ion ratios can reflect changes in volcanic activity (de Hoog et al., 2001), and the compositions of leachates from volcanoes in the same region tend to be similar due to shared magma types (Giggenbach, 1996). The adsorption of volatiles into ash represents a significant sink, often overlooked in volatile budget calculations, and standardizing leachate analysis techniques is crucial for accurate comparisons and environmental applications (Witham et al., 2005).

Another important process through which volcanic eruptions affect freshwater resources involves the interaction between surface water and/or groundwater with upward volcanic fluids, such as gases and hydrothermal solutions, resulting from the reactivation of the underlying hydrothermal system (Armienta et al., 2008; Giammanco et al., 1998). In this scenario, ascending fluids released from magma chambers play a significant role in hydrogeochemical processes, leading to the dissolution of the hosting rocks, enhanced by dissolved CO2 or temperature increase. This water-rock interaction process often leads to increased concentrations of RFEs (Rock forming elements), Na, Ca, K, SiO2 (Varekamp, 2008) and trace elements, including Li, Mn, Si, V, As, Mo, Al, Fe, Ni, B, Se, Co, and Hg, not only in the ascending fluids but also in the groundwater when they mix with near-surface volcanic aquifers (Giammanco et al., 1998). Alongside the fluids, gases such as CO_2, SO_2, HCl, and HF, among others, also ascend and get trapped or dissolved in the volcanic aquifers, leading to hydrochemical variations in the groundwater. The analysis of these trapped gases provides valuable information on the heat and gas transfer dynamics occurring in both dormant and erupting volcanoes (Allard et al., 1997; Parello et al., 2000; Sorey et al., 1993).

The impact of volcanic gases on the chemical composition of groundwater is dependent on the alteration of volcanic stress patterns, which can result from either magma displacements or the release of strain through volcano-tectonic earthquakes (Lachowycz et al., 2013). The emplacement of magma domes facilitates the leaching of host rocks, primarily promoting the weathering of ferromagnesian minerals (Armienta et al., 2008). In some cases, the changes are more related to seismic activity near the volcano, indicating groundwater flowing through new paths influenced by the stress field and/or seismic fracturing. (Armienta and De la Cruz-Reyna, 1995). Under extreme scenarios during the eruption, fluid coming from the hydrothermal system may get through aquifers and interact directly with surface water bodies, e.g., heating a lake water temperature up to 58 °C and generating extremely acid pH of 0.5 (Casadevall et al., 1984). The changes in concentration of chemical species can result from either direct interaction of diffuse fluids released from magma chambers with aquifers or the creation of new pathways for water and gases due to reactivation of the fault system. Short-term fluctuations in water chemistry, such as changes in chloride, boron, and sometimes fluoride and sulfate concentrations, are likely caused by the interaction of available magmatic gases with water or newly exposed fault surfaces, i.e., freshly exposed rock. Fresh or unaltered rock exposed to hydrothermal fluids or groundwater can undergo mineral dissolution and precipitation, which result in a water composition change (Karakaya et al., 2012). Conversely, slow trends in sulfate and CO_2 concentrations suggest that these chemicals are gradually accumulating through scrubbing of diffuse or fault-transported volcanic gases that exhibit significant variations in open vents. Reductions in their concentrations near the peak of magmatic activity suggest that the source magma-mixing process is declining (Armienta et al., 2008).

Boron, chloride, sulfate, fluoride, and CO_2 are chemical species that exhibit high sensitivity to variations in volcanic activity (De la Cruz-Reyna and Tilling, 2008; Garlick and Wedepohl, 1969; Silva et al., 2000). Assessing the production of volcanic CO_2 in the gas phase of volcanoes is challenging due to its intermittent nature, with measurements during bursts yielding varying results. However, CO_2 accumulation in groundwater can help mitigate rapid fluctuations and provide an

estimate of the mean production rate of volcanic CO_2 (Fischer et al., 2019). During periods of increased magmatic activity, the supply of CO_2 may come from either magmatic gases or produced by limestone-derived CO_2 assimilation (Federico et al., 2002). The assimilation of limestone into the magma has been proposed to occur at depths of several kilometres beneath the volcano summit to explain high CO_2 discharge events, with a CO_2 flux occasionally exceeding 100,000 tons per day (Goff et al., 2001). The absence of diffuse CO_2 in the soils surrounding young volcanoes suggests that the transport of CO_2 predominantly takes place through the main vent and the surrounding fracture system. Consequently, it has been proposed that a portion of these CO_2 bursts might accumulate in groundwater, resulting in the gradual increase observed in some springs (Varley and Armienta, 2001).

Previous studies have reported the observation of boron peaks preceding or occurring simultaneously with increased volcanic activity at various Mexican volcanoes, including Colima (Armienta and De la Cruz-Reyna, 1995; Silva et al., 2000) and Tacaná (De la Cruz-Reyna et al., 1989). In the case of Colima, boron peaks were associated with dome growth and explosive events, while at Tacaná, it was linked to a phreatic explosion. Similar evidence of volcanic gas scrubbing in aquifers leading to boron input has also been documented at Mount Etna (Giammanco et al., 1998).

Armienta et al. (2008) reported that a fluoride concentration peak was observed at several springs close to the Popocatépetl volcano coinciding with its second stage of the magma output. The authors proposed that this phenomenon could be attributed to an elevation in the release of HF, which is known to be one of the most soluble gases found in magma (Scarpa et al., 1996). This increase in HF emissions would occur during the later stage of heating within magma chambers, particularly when the highest temperatures are most prevalent.

Despite the considerable risks that volcanic eruptions entail to water resources, there has been a limited focus on the impact on groundwater in volcanic islands. Regarding the volcanic activity in the Canary Islands, Padrón et al. (2020) conducted a study to assess the potential impact on groundwater supply of a submarine volcanic eruption in *El Hierro* (Canary Islands) in 2012, monitoring the metal and trace element concentrations. The results indicated that the groundwater samples maintained the quality standards for human consumption outlined in Spanish legislation (RD 140/2003), despite the volcanic eruption. However, this eruption occurred underwater, two away km from the island, without directly affecting freshwater, unlike the aerial eruption of Tajogaitein (2021) in La Palma Island.

This paper aims to address this research gap by presenting a study that specifically investigates the effects on groundwater resources of the volcanic eruption in 2021 in *La Palma* Island. This study serves as the second part, building upon the work conducted by García-Gil et al. (2023), which focused on the hydraulic impacts of the volcanic eruption. In this second part, the research investigates the hydrogeochemical resilience of groundwater resources to volcanic eruptions through the analysis of major, minor, and trace elements in solution obtained from deep piezometers, wells, springs, and drainage galleries. The investigation extends throughout the duration of the eruption and into the post-eruption phase, covering a period of one year after the volcanic event. The results obtained were then compared with historical hydrochemical analysis from the local water authority to assess the magnitude of the impacts. This aspect of volcanic eruptions, particularly the interaction with ash leachates, has received less investigation compared to surface water bodies. Thereby, the results of this work aim to have significant implications for water resource management and sustainability in volcanic islands, particularly in regions where groundwater is the primary source of freshwater.

2. Study area

The volcanic island of *La Palma*, which is an active volcanic system, stretches 47 km from north to south and 29 km from east to west. It is situated at the northwest extremity of the Canary Islands volcanic chain, which extends for 500 km off the northwest coast of Africa (Fig. 1). *La Palma* is characterized by a stratovolcano that rises approximately 6500 m above the seafloor, developed on Jurassic-age oceanic crust (Hayes and Rabinowitz, 1975). The island is notable for its volcanic stratigraphic structures (De la Nuez et al., 2008) consisting of two distinct units (Hiltona et al., 2000): the Seamount Series (4–2.9 Ma) and the subaerial complex known as the *Coberta Series* (2.0–0.0 Ma). With the exception of gabbroic outcrops of the Seamount Series found at the base of the *Caldera de Taburiente*, the *Coberta Series* covers the entire island. The latter series comprises two subunits: the main shield volcano in the north of the island (2.0–0.6 Ma), and a more recent subunit (0.6–0.0 Ma) consisting of lavas forming at the southern *Cumbre Vieja* ridge (Ancochea et al., 1994; Guillou et al., 1996). In addition, the island exhibits a locally erosive and intermittent feature called the *COEBRA* structure (Navarro Latorre, 1993). This structure is located within the northern shield volcano and contains numerous springs, some of which have significant flow rates (APHP, 1992).

The island of *La Palma* features a complex volcanic aquifer system, mainly consisting of basaltic lavas with pyroclastic layers in between. This system is divided into blocks by dykes generating a dyke-impounded system. These dykes compartmentalize the hydrogeological system in which the flow of groundwater is blocked or slowed by a volcanic dike and control groundwater flow direction and density based on their proximity to *La Palma's* structural axes (Poncela et al., 2022). The resulting sealing cells act as hydrological barriers and cause high local piezometric gradients. The presence of debris avalanche deposits that resulted from gravitational landslides can also affect the confinement or semi-confinement of the island's groundwater bodies (Poncela, 2009, 2015). Groundwater follows a flow regime from the summit towards the sea, but the presence of dykes hinders its movement, causing it to reach the regional groundwater levels at around 1800 m inland and sea level in the coastal zone (Custodio, 2020).

The primary groundwater reservoir, defined as LP001 groundwater body according to the WFD 2000/60/EC directive, encompasses *La Palma's* primary insular aquifer system, the *Taburiente* volcano cone components, and the *COEBRA* structure (APHP, 1992; APPHLP, 2012; EGDHLP, 2009). It stretches from the northern cone halfway to the southern cone and down to the coastal fringe, reaching a benchmark of 600 m. a.s.l. Although the stacked lava and scoria layers from the upper *Taburiente* volcano ensure infiltration and natural recharge to the main aquifer, permeability presents noticeable contrast due to lithological heterogeneity like the overlaid series, acting as a low permeability basement that can either cut across or be in contact with the *COEBRA* or Basal Complex structures. *La Palma* features two primary flow regimes, a regional flow regime that contains groundwater that was recharged decades or centuries ago and a local flow regime at elevations above 1000 m. a.s.l. Characterized by high Tritium contents, low mineralization, and low groundwater residence times. Additionally, the water stratification processes, which primarily occur at upper levels of the aquifer, are vital in *La Palma's* water recharge system. The debris avalanche scars are true erosive landforms of lopsided caldera basins, serving as precursors to the island's groundwater reservoirs (Poncela and Skupien, 2013).

3. 2021 eruption of the *Tajogaite* Volcano

The 2021 eruption of the *Tajogaite* volcano on *La Palma* Island was characterized by typical Strombolian activity, featuring alternating phases of explosive eruptions expelling pyroclastic material and effusive phases with lava emissions. According to the official reports from the special plan of civil protection and emergency response for volcanic risk in the Canary Islands (PEVOLCA, 2021), the magma emerged through a 557-m-long fissure with a northwest-southeast orientation. Lasting 85 days, the eruption resulted in the opening of six vent centers (Fig. 1). A prominent cone composed of pyroclastic material, reaching a height of

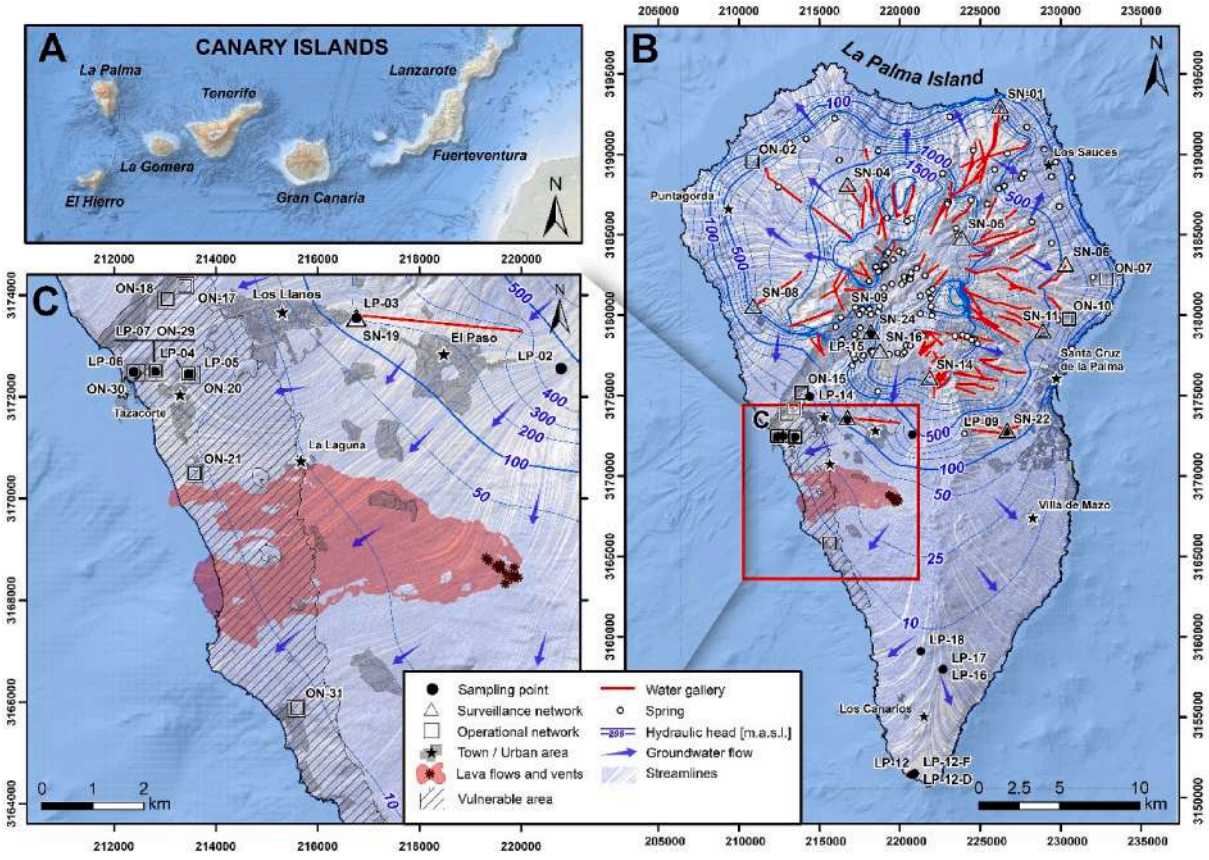

Fig. 1. Study area. Location of (A) *La Palma* Island in the Canary Islands archipelago; (B) *La Palma* Island groundwater head contour map from Poncela (2015); and (C) The *Aridane - Tazacorte* Valley and *Tajogaite* Volcano (2021). Projection: REGCAN95/UTM zone 28 N. Bathymetric map backgrounds obtained from the European Marine Observation and Data Network (EMODnet) in A and the *IHM - Instituto Hidrográfico de la Marina – Armada* in B and C.

200 m, formed during the eruption, with the overall volcanic structure reaching an elevation of 1100 m above sea level. The majority of the emitted lava from *Tajogaite* volcano was viscous (<900 °C), resulting in *aa*-type or rough blocky lava flows moving at rates of meters per minute. At the same time, the volcano emitted less viscous and more fluid lava, leading to smoother pahoehoe surface flows. These flows moved rapidly, reaching speeds of meters per second, and had higher temperatures than the *aa*-type lava flows, with maximum readings of 1140 °C. The lava flows covered an area exceeding 1200 ha, spanning a distance of over 6.5 km from the main cone and reaching the coastline in three different locations (Fig. 1). The eruption on La Palma gave rise to two types of volcanic rocks: tephrites, consisting of approximately 50% volcanic glass and crystals of pyroxene, amphibole, plagioclase, and iron and titanium oxides, and basanites, which contained olivine crystals.

Water vapor was the most abundant gas emitted during the eruption of *Tajogaite* volcano, followed by CO_2, SO_2, CO and AsH_3. Around two million tons of SO_2 were emitted during the eruption, resulting in two episodes of acid rain. Gases released by the magma escaped through fractures or fumaroles formed around the volcano cone, leading to the deposition of sulfur and NH_4Cl compounds. During the eruption, water vapor columns mixed with lighter-colored ash clouds were observed and related to rising magma interaction with groundwater bodies, resulting in highly explosive phreatomagmatic eruptions and the production of phreatomagmatic breccias.

4. Methodology

4.1. Data collection, monitoring and water sampling campaigns

The Insular Water Authority of *La Palma* (*Consejo Insular de Aguas de La Palma*, CIALP) has established two networks for monitoring the chemical state of groundwater resources on the island - an operational and a surveillance network (Fig. 1). The surveillance network comprises 12 representative water galleries and one piezometer, and is employed to monitor the general trends of the hydrochemical parameters of the groundwater. On the other hand, the operational network comprises 11 representative wells located in specific areas where potential contamination risks exist. Additionally, the CIALP manages a piezometer network consisting of 12 monitoring points that has been established to monitor the quantitative state in the most intensively exploited and vulnerable area of the *Aridane-Tazacorte* Valley (Fig. 1C). In response to the *Tajogaite* eruption on September 19th, 2021, the Geological Survey of Spain (IGME) established a 15 point-monitoring network to assess the possible impact of the eruption on groundwater resources (Table 1). For this purpose, three sampling campaigns involving a total of 35 groundwater samples were conducted. The first one was performed during the eruption (9 samples) and the other two after the eruption, six months (14 samples) and one year (12 samples) after the eruption, i.e., October 2021, June 2022 and December 2022, respectively. The concentrations of major cations (Ca^{2+}, Mg^{2+}, Na^{+} and K^{+}), anions (Cl^{-}, NO_3^{-}, SO_4^{2-}, F^{-} and HCO^{3-}), silica (SiO_2) and trace elements (Al, As, Ba, Be, B, Cd, Co, Cr, Cu, Fe, Hg, Mn, Mo, Ni, Pb, Sb, Se, Sr, V, Zn, Tl, Th, and U) of the 35 groundwater samples were analyzed. During each field campaign, in-situ physicochemical parameters including electrical conductivity (EC), temperature (T), pH and dissolved oxygen (DO) were measured. The in-situ physicochemical parameters were measured using portable meters (HACH HQ4300 PHC20101/CDC40101/LDO10101). Filtered water samples (0.45 μm) were carefully transferred into high-density polyethylene (HDPE) bottles. Specifically, for preserving anion samples, HDPE bottles with a capacity of 250 ml were employed, while HDPE bottles with a volume of 125 ml were utilized for cation analysis. Cation and silica samples were acidified with HNO_3 (1.6 N) to pH < 2

Table 1
Data summary for volcanic eruption campaigns conducted by the authors (IGME) and provided by the Insular Water Authority (CIALP) and the Spanish Geological Survey database (IGME DB).

Label	Type	Pre-Eruption Author(s) (n° samples)	During-Eruption Author(s) (n° samples)	Post-Eruption Author(s) (n° samples)	Total Number of samples	Date Range of Data Availability		Distance to Volcano [km]
LP-02	Piezometer		IGME (1)	IGME (2)	3	18/10/2021	12/12/2022	4.0
LP-03	Water gallery	CIALP (20)	IGME (1), CIALP (1)	IGME (2)	24	01/02/2014	12/12/2022	5.4
LP-04	Piezometer		IGME (1)	IGME (2)	3	18/10/2021	12/12/2022	6.9
LP-05	Well	IGME DB (18), CIALP (10)	IGME (1), CIALP (1)	IGME (2), CIALP (1)	33	07/05/1969	12/12/2022	6.8
LP-06	Well	CIALP (9)	IGME (1), CIALP (1)	IGME (2), CIALP (1)	14	28/05/2014	12/12/2022	7.8
LP-07	Well	IGME DB (21), CIALP (9)	IGME (1), CIALP (1)	IGME (2), CIALP (1)	35	28/01/1976	12/12/2022	7.5
LP-09	Water gallery	CIALP (2)	IGME (1)	IGME (2)	5	02/09/2019	13/12/2022	7.9
LP-12	Spring		IGME (1)		1	19/10/2021	19/10/2021	16.9
LP-12D	Water gallery			IGME (2)	2	28/07/2022	12/12/2022	16.8
LP-12F	Water gallery			IGME (2)	2	28/07/2022	12/12/2022	16.8
LP-14	Surface water collector		IGME (1)	IGME (2)	3	19/10/2021	12/12/2022	7.8
LP-15	Spring	CIALP (1)		IGME (1)	2	30/09/2019	29/07/2022	10.1
LP-16	Spring			IGME (2)	2	28/07/2022	12/12/2022	10.7
LP-17	Spring			IGME (2)	2	28/07/2022	13/12/2022	10.7
LP-18	Spring			IGME (1)	1	28/07/2022	28/07/2022	9.4
ON-02	Well	CIALP (3)			3	01/10/2019	23/04/2021	22.3
ON-07	Well	CIALP (3)			3	02/09/2019	13/04/2021	18.8
ON-10	Well	CIALP (3)			3	02/09/2019	13/04/2021	15.3
ON-15	Well	CIALP (3)		CIALP (1)	4	04/09/2019	02/12/2022	8.4
ON-17	Well	CIALP (3)	CIALP (1)	CIALP (1)	5	04/09/2019	02/12/2022	8.0
ON-18	Well	CIALP (2)		CIALP (1)	3	11/08/2020	01/12/2022	8.0
ON-21	Well	CIALP (3)		CIALP (1)	4	04/09/2019	02/12/2022	6.0
ON-31	Well	CIALP (3)			3	20/10/2019	06/04/2021	4.8

and stored at a constant temperature of 3 °C. The samples were transported by plane under refrigerated conditions and delivered to the laboratories of the Spanish National Geological Service within 24 h after the last groundwater sample was obtained. The analysis of major elements was conducted using Inductively Coupled Plasma-Optical Emission Spectrometry (ICP-OES) with an Agilent 5800 instrument. The analysis of trace elements was performed using Inductively Coupled Plasma-Mass Spectrometry (ICP-MS) with an Agilent 7500ce instrument following the EPA Method 200.8. Due to the uncertainty associated with volcanic eruptions, there was no hydrochemical survey conducted before the eruption. Consequently, historical geochemical analysis from the Insular Water Authority (CIALP) and analysis from the IGME groundwater database were considered to assess the impacts of the eruption on groundwater composition. In-situ measurements of the physicochemical parameters EC, pH, and T were obtained from CIALP using the RINKO AAQ171 multiparameter probe (ECOS-01-RIN). The historical hydrochemical analysis provided by CIALP for this study used various analytical techniques. Bicarbonates (HCO_3^-) and alkalinity were analyzed using a Metrohm Titrator. The major cations, including Ca, Mg, K, and Na, were analyzed using ICP-MS method. The analysis of anions involved the use of different techniques: Cl^-, F^-, NO_3^- and SO_4^{2-} were analyzed using HPLC-Conductivity method, while PO_4^{3-} was determined using Spectrophotometry (Absorption). Finally, trace elements Al, Sb, As, B, Cd, Cu, Cr, Fe, Mn, Hg, Ni, Pb, and Se were analyzed using the ICP-MS method. The laboratory providing services to CIALP holds accreditation from the Spanish National Accreditation Body (ENAC n° 109/LE285). Finally, the charge balance error of the water analyses was calculated with PHREEQC (Parkhurst and Appelo, 2013) in order to determine the reliability of the analysis results for each sample.

4.2. Statistical analysis

Statistical analysis was performed with the software SPSS v25.0 (IBM Corp., 2017). The means for the different parameters studied were compared before, during and after the eruption (eruption phase independent variable) using different statistical tests. Normality of distribution and homogeneity of variances were assessed using Kolmogorov-Smirnov and Levene's tests, respectively. Mann–Whitney test (when only two means were compared) or Kruskall-Wallis test plus post-hoc tests (when more than two means were compared) were used, as the data did not meet normality, homogeneity of variances or sphericity assumptions. p values < 0.05 were considered to indicate statistical significance (*), p values below 0.01 were considered as high statistical significance (**) and p values below 0.001 indicated very high statistical significance (***). In addition, p values between 0.05 and 0.08 were considered as tendencies to statistical significance, and discussed where considered relevant.

Subsequently, a multivariate two-way MANOVA test was performed to determine the combined impact of the independent variables: geographical location and eruption phase (pre-eruption, eruption and post-eruption) on the dependent variables (the different parameters studied). Statistical significance was established at the $p < 0.01$ level. General significant correlation between dependent variables was assessed and confirmed before performing the multivariate statistical analysis, since meeting this assumption is needed to implement a multivariate analysis.

Sperman's *rho* coefficients were calculated to determine potential correlations impacts on the trace element concentrations and distance to the volcano.

5. Results and discussion

5.1. Chemical analysis results and exploratory assessment of the groundwater hydrochemistry

Physicochemical parameters measured and chemical analysis results

of groundwater samples for volcanic eruption stages: pre-eruption (PRE), eruption (ERUP), and post-eruption (POST) at the 155 sampled monitoring points are provided as supplementary material (Tables S1 and S2). Fig. 2 displays major ions from the analysis with a charge balance error percentage below 10% (following the admissible error criteria proposed by Zhu et al., 2002) projected onto a Piper diagram. The diagram illustrates the hydrochemical compositions before, during, and after the volcanic eruption. Except for some chloride-rich samples, the diagram clearly shows a dominant sodium bicarbonate facies, although a higher variability is observed in the eruption and post-eruption samples. The Mg/Ca ratio remained relatively constant at approximately 1.00 ± 0.35 (outliers were defined as values beyond ±3 standard deviations) across all samples collected during the eruption stages. A constant Mg/Ca ratio may indicate stability in the water-rock interaction processes (e.g. by thermodynamical equilibrium with the most soluble Mg-rich and Ca-rich minerals of the hosting basaltic rocks such as plagioclases and pyroxene). Minerals that are often found in basaltic rocks and commonly exhibit a constant Mg/Ca ratio include plagioclase feldspars, pyroxenes, and amphiboles. Common amphibole minerals found in basaltic rocks include hornblende and actinolite, which can exhibit a constant Mg/Ca ratio in volcanic rocks. During the eruption and post-eruption stages, samples presenting low (<50%) Na + K contents were clearly modified but still maintaining a Mg/Ca ratio giving a "Y" Shape. Anions also showed a "Y" shape with the majority of the samples matching the bicarbonate type facies and also showing a constant SO_4/Cl ratio of 0.38 ± 0.09 (outliers were defined as values beyond ±3 standard deviations) across all samples collected during the eruption stages. Since S is not a rock-forming-element in basaltic rocks, its increase in solution is prone to originate from various sources related to volcanic activity, mainly from magma degassing, from a possible infiltration of water with higher SO_4/Cl ratio, such as a deep hydrothermal fluid or, to a lesser extent, from interaction with rocks containing sulfide minerals. Chlorine can come from seawater, hydrothermal fluids, or other sources. Magmatic degassing leads to the release of volatile components, including CO_2 that would increase the aggressive character of the rising fluids, thereby increasing the dissolution of basaltic rocks minerals. That would explain the arms of the "Y" shape as the concentrations are increased while the mentioned ratios are maintained almost constant.

The temporal changes in minor and trace elements during the three distinct eruption stages are shown in Fig. 3. Taking into account the threshold values for human drinking quality standards (EPA, 2001; EPA, 2009; WHO, 2004; WHO, 2011), it can be observed that several trace elements already exceeded guidelines threshold values before the investigated eruption. This was observed for Al, Fe, Mn and Sb, although these exceeding concentrations are mainly detected in a few samples. During the eruption, Al was clearly increased in LP-02 and LP-04 reaching, but not significantly exceeding, the 200 μg L^{-1} threshold value. The EPA 600 μg L^{-1} threshold value for B is only exceed by LP-15. Since this sampling point coincides with a borehole in the submarine edifice, i.e., the low permeability basement of the island, it involves the contribution of a deep hydrothermal water cooled during the ascent with high pCO_2 and already high Fe contents (>1 mg L^{-1}). This sampled point showed a valuable information on the possible reactivation or

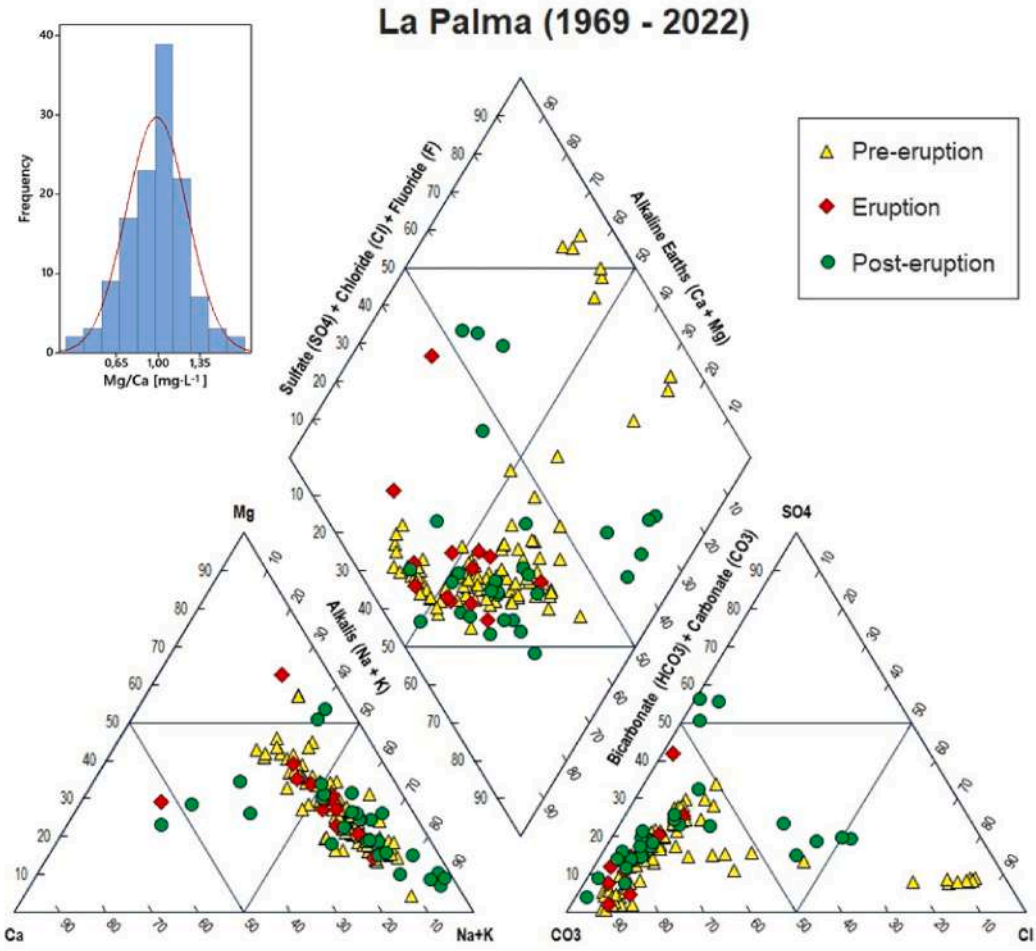

Fig. 2. Piper diagram depicting alterations in hydrochemical composition (mg·L^{-1}) prior to, during, and following the eruption. The diagram exclusively represents samples exhibiting a charge balance error percentage below 10%.

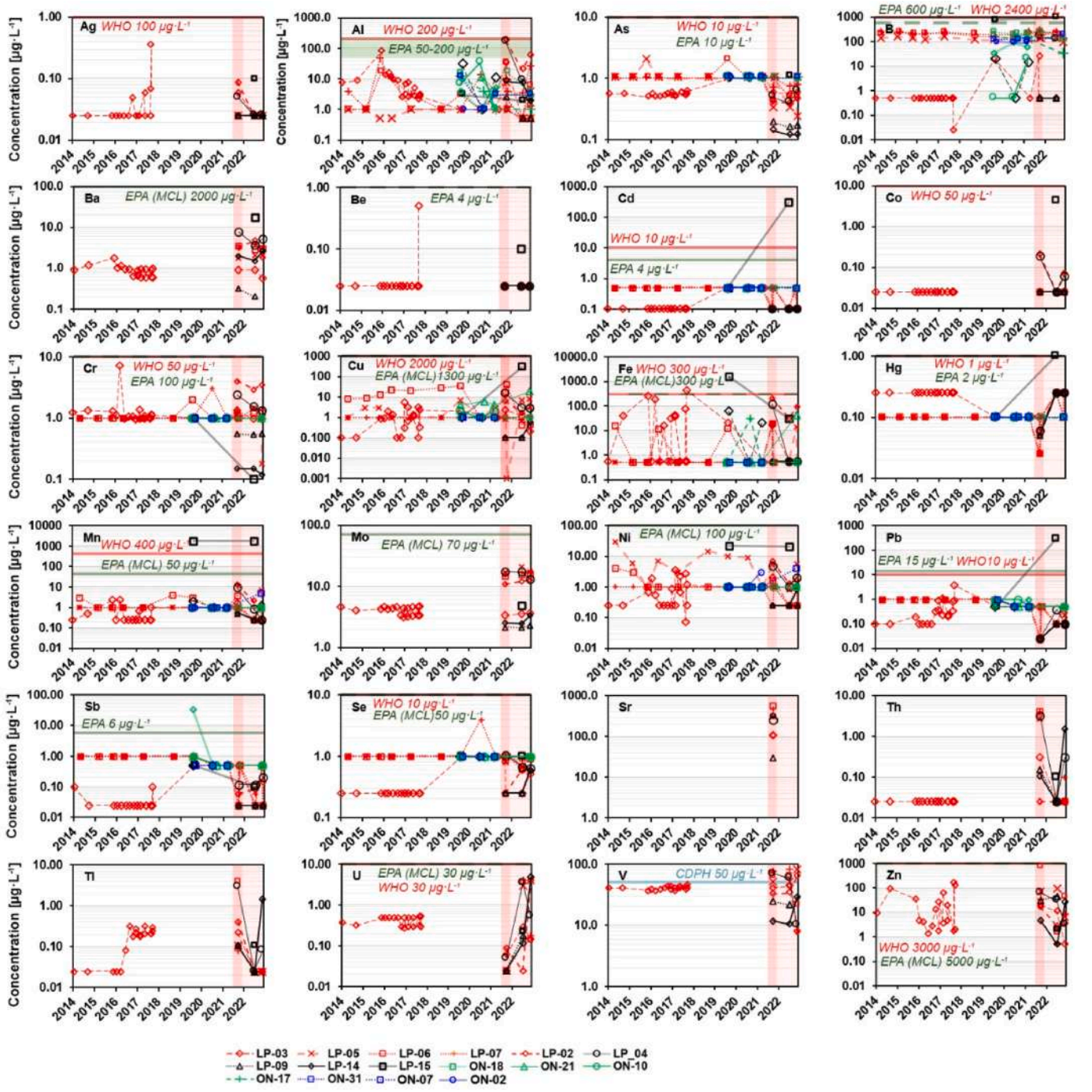

Fig. 3. Temporal evolution of minor and trace elements along three distinct eruption stages differentiated: pre-eruption, eruption, and after the eruption. Drinking water quality standards are displayed (EPA, 2001; EPA, 2009; WHO, 2004; WHO, 2011).

enhancement of the hydrothermal convection cells with an increase of Cu, Cd, Hg and Pb of several orders of magnitude, far above the recommended threshold values (excepting Cu).

A detailed review of the trace elements change from Fig. 3 where this changes can be identified is provided in Table 2. Variations are indicated as both absolute maximum change in $\mu g \cdot L^{-1}$ and relative change in percentage increase. The evaluated impacts showed that Sr increase values range between 273 ± 185 µg L^{-1} (54,550%) in average increments, with a maximum of 564 µg L^{-1} (112,800%) at LP-06, which is located near the coast. The group of trace elements of Al, V and Fe presented a variation range of 45 ± 47 µg L^{-1} (2047%) on average. A relatively low variation of 5 ± 5 µg L^{-1} (4321%) on average was found also for Cu, U, Ni. Th, Ba, Tl and Cr. Finally, Hg, As and Ag showed increments of 0.12 ± 0.09 (220%) $\mu g \cdot L^{-1}$ on average.

The statistical correlation analysis provided insights into the relationship between hydrogeochemical impacts on each trace element and the distance of the monitored point sampled to the volcano. These correlations are provided in Table 3. First, negative correlations were found for Ag, Al, As, Ba, Cr, Cu, Fe, Hg, Ni, Th, Tl, U, and V, suggesting that hydrogeochemical impacts on these elements tend to decrease as the distance from the erupted volcano increases, and viceversa. One possible explanation is that the volcano eruption would release and disperse these elements into the surrounding environment, causing higher concentrations closer to the volcano. As the distance increases, dispersion

Table 2
Absolute and relative hydrogeochemical impacts of each analyzed trace element at sampled monitoring points.

Monitoring point	Absolute hydrogeochemical impact [μg·L^{-1}]													
	Ag	Al	Sr	As	Ba	Cr	Cu	Fe	Hg	Ni	Th	Tl	U	V
LP-02	0.065	154.00	112.0	0.07	2.94	3.89	5.17	112.70	0.19	5.68	0.00	0.39	3.86	56.12
LP-03	0.035	31.40	113.0	0.03	0.34	0.35	2.16	17.40	0.19	1.74	0.29	0.20	0.27	34.72
LP-04	0.025	162.81	262.0	0.21	4.09	1.08	12.17	119.45	0.19	3.91	3.11	2.83	3.43	61.82
LP-05		6.90	306.0	0.30	1.80	1.22	7.14	19.20	0.23	4.99	2.68	0.08	4.15	71.82
LP-06		30.80	564.0	0.06	0.66	0.19	42.57	19.00	0.23	1.41	4.00	4.00	3.60	57.62
LP-07		5.30	481.0	0.10	0.61	0.92	0.33	0.10	0.28	0.00	3.78	0.08	3.94	73.70
LP-09		1.86	30.2	0.03	0.11	0.01	0.00	0.00	0.20	0.00	0.13	0.08	0.15	16.22
LP-14		6.20	314.0	0.02	1.13	0.03	0.45	0.00	0.20	0.57	1.48	0.08	4.71	18.90
ON-17							0.00	0.00	0.00	0.00				
ON-18							0.00	0.00	0.00	0.00				
ON-21		0.00					15.00	41.45	0.00	3.75				
Monitoring point	**Relative hydrogeochemical Impact [%]**													
	Ag	**Al**	**Sr**	**As**	**Ba**	**Cr**	**Cu**	**Fe**	**Hg**	**Ni**	**Th**	**Tl**	**U**	**V**
LP-02	260	770	22,400	18	164	38,900	502	121	317	427	0	1540	15,420	703
LP-03	140	6280	22,600	5	61	37	1080	3480	317	696	1140	780	1060	435
LP-04	100	7434	52,400	54	113	82	446	21,718	317	387	12,420	11,300	13,700	775
LP-05		690	61,200	150	800	678	830	3840	900	594	10,700	300	16,580	900
LP-06		1027	112,800	14	23	19	9900	3800	900	564	15,980	15,980	14,380	722
LP-07		133	96,200	14	20	184	56	20	1100	0	15,100	300	15,740	899
LP-09		62	6040	7	4	1	0	0	800	0	500	300	580	203
LP-14		307	62,800	17	75	25	450	0	400	228	5900	300	18,820	182
ON-17							0	0	0	0				
ON-18							0	0	0	0				
ON-21		0					375	7536	0	1500				

and dilution processes occur, leading to lower concentrations and, thus, weaker hydrogeochemical impacts. On the other hand, the positive correlation found for Sr implies that Sr levels tend to increase as the distance from the erupted volcano increases, and viceversa (Fig. 5 and Fig. 6). One possible explanation would be that Sr, that commonly shows higher values in seawater, could be released into groundwater through the mixing between a mixture of seawater and hydrothermal fluids, since this already occurs in the thermal spring Fuente Santa, located in the island. A strong negative correlation is evidenced between Ag and Al, as well as between Sr and Th, so that when the concentration of Ag increases, the concentration of the other one decreases, and viceversa. Al and Tl tend to be correlate positively ($r = 0.81$), as well as Sr with Th ($r = 0.79$). A positive correlation was also found between As and Cu ($r = 0.71$), Fe ($r = 0.76$), Tl ($r = 0.82$) and V ($r = 0.71$). Fe also correlated positively with Cr ($r = 0.85$), Cu ($r = 0.6$) and Ni ($r = 0.83$). Active volcanic islands often experience hydrothermal activity, which involves the circulation of hot water through volcanic rocks. This hydrothermal water can interact with the basaltic rocks, dissolving minerals containing Fe, Cr, Cu, and Ni, that are released into the groundwater (Appelo and Postma, 2005). On the other hand, magmatic fluids, originating from the molten magma chambers beneath the volcanic island, can migrate through fractures and fissures in the rocks, reaching the groundwater. These fluids can also carry elevated concentrations of Fe, Cr, Cu, and Ni, contributing to their presence and association in groundwater. Thus, the mentioned correlations suggest the interaction between fresh groundwaters and hydrothermal fluids, as a diffuse interaction affecting several water sampling points in the island. Finally, Cu shows a strong positive correlation with Hg ($r = 0.69$), Ni ($r = 0.71$), Th ($r = 0.70$), Tl ($r = 0.81$) and V ($r = 0.81$). This trace element association is common in aqueous environments since they exhibit similar sources, mobility, or affinity for certain minerals, which can lead to their co-occurrence and strong correlations in groundwater. Redox conditions in groundwater can influence the mobility and speciation of these elements. They can undergo complex redox reactions, and their correlation may indicate similar and stable redox conditions favouring their co-occurrence and solubility (Langmuir, 1997).

Several trends of the trace element variations in relation to the distance to the volcano are presented in Fig. 4 for each trace element investigated (see Fig. 5).

Table 3
Correlation matrix resulting from the statistical analysis of the different hydrogeochemical impacts investigated and its distance to the volcano *Tajogaite*. Spearman's rho correlation coefficient for nonparametric correlations is given. Data values with a 0.05 significance level are indicated in bold. Correlations significant at the 0.05 (*) level (2-tailed) and correlations significant at the 0.01 (**) level (2-tailed) are given.

Variable	Distance	Ag	Al	Sr	As	Ba	Cr	Cu	Fe	Hg	Ni	Th	Tl	U	V
Distance	1.00														
Ag	**−1.00****	1.00													
Al	−0.18	**−1.00***	1.00												
Sr	0.67	**−1.00***	−0.43	1.00											
As	−0.34	−0.50	0.76	−0.49	1.00										
Ba	−0.28	−0.50	0.19	−0.17	0.51	1.00									
Cr	**−0.85****	0.50	−0.02	−0.43	0.41	0.38	1.00								
Cu	−0.52	−0.50	0.57	0.05	**0.71***	0.48	0.45	1.00							
Fe	**−0.76****	−0.50	0.18	−0.55	**0.76***	0.49	**0.85****	**0.60***	1.00						
Hg	−0.40		0.15	0.43	−0.10	−0.05	0.48	**0.69***	0.27	1.00					
Ni	**−0.84****	0.50	0.17	−0.59	0.67	0.40	**0.81**	**0.71***	**0.83****	0.31	1.00				
Th	−0.14	**−1.00****	0.28	**0.79***	−0.10	0.14	−0.05	**0.70**	0.12	**0.88****	0.15	1.00			
Tl	−0.42	−0.50	**0.81****	−0.15	**0.82***	0.60	0.24	**0.81****	0.37	**0.69***	0.49	**0.72***	1.00		
U	−0.32	0.50	−0.23	0.40	−0.41	0.24	0.29	0.58	0.00	**0.72***	0.34	**0.70***	0.49	1.00	
V	−0.47	−0.50	0.65	−0.19	**0.71***	0.10	0.60	**0.81****	0.47	**0.76****	**0.64***	**0.69***	**0.82****	0.56	1.00

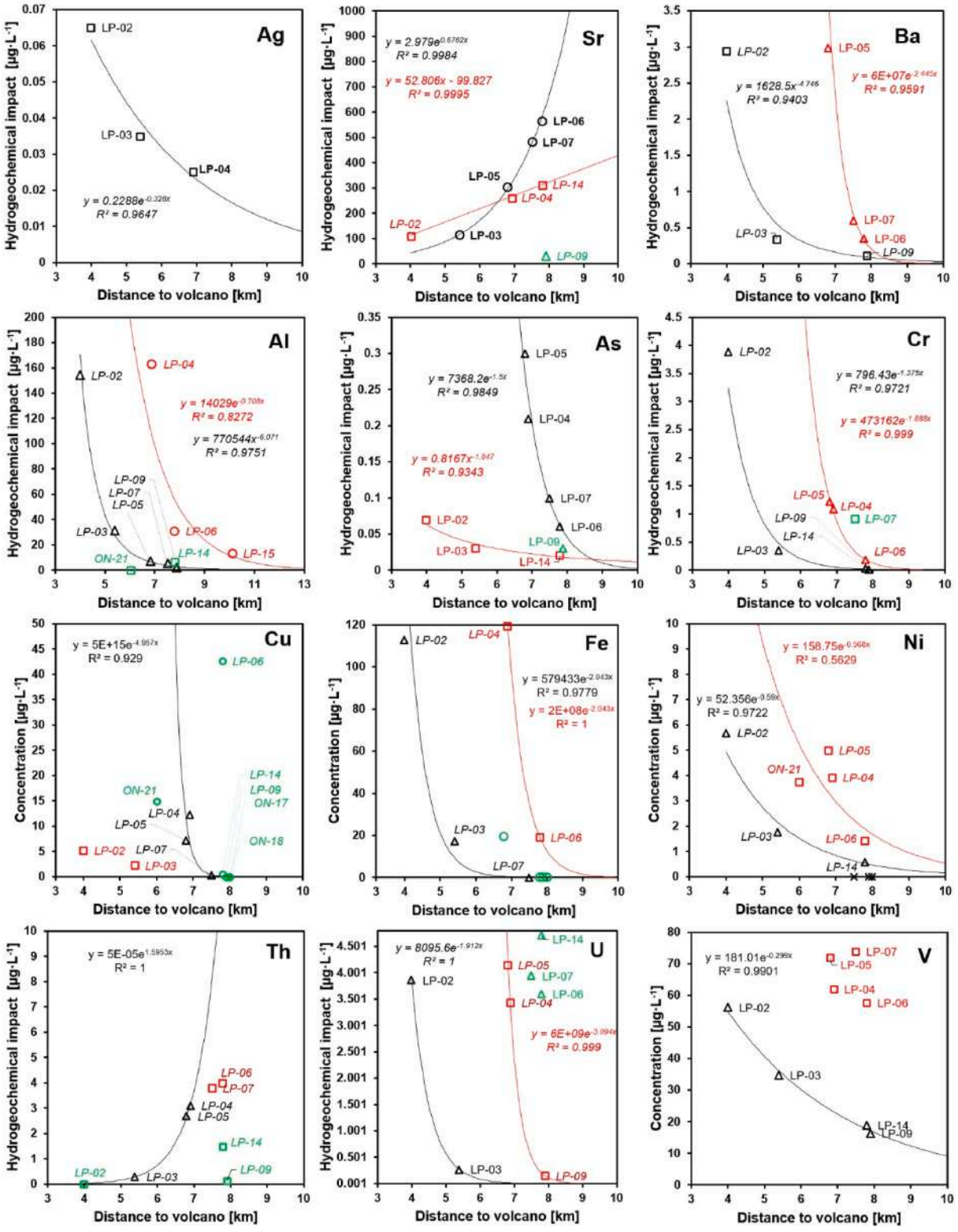

Fig. 4. Hydrogeochemical impacts for each trace element investigated and possible distributions in relation to their distance to the volcano.

5.2. Statistical analysis results

5.2.1. Univariate analysis of the effect of the eruption phase on the studied parameters

The univariate statistical analysis conducted revealed significant differences among various parameters, based on the effect of the independent variables on them (sample location and eruption phase) (Table 4). Further post-hoc statistical analysis showing the multiple comparisons is shown in Table S1.

Figs. 7 and 8 shows the means for the three eruption phases studied. With regard to the general parameters studied, the Kruskall-Wallis and subsequent post hoc tests performed indicated that the differences observed in temperature means among the three eruption phases were statistically significant ($p = 0.006$), with temperature values

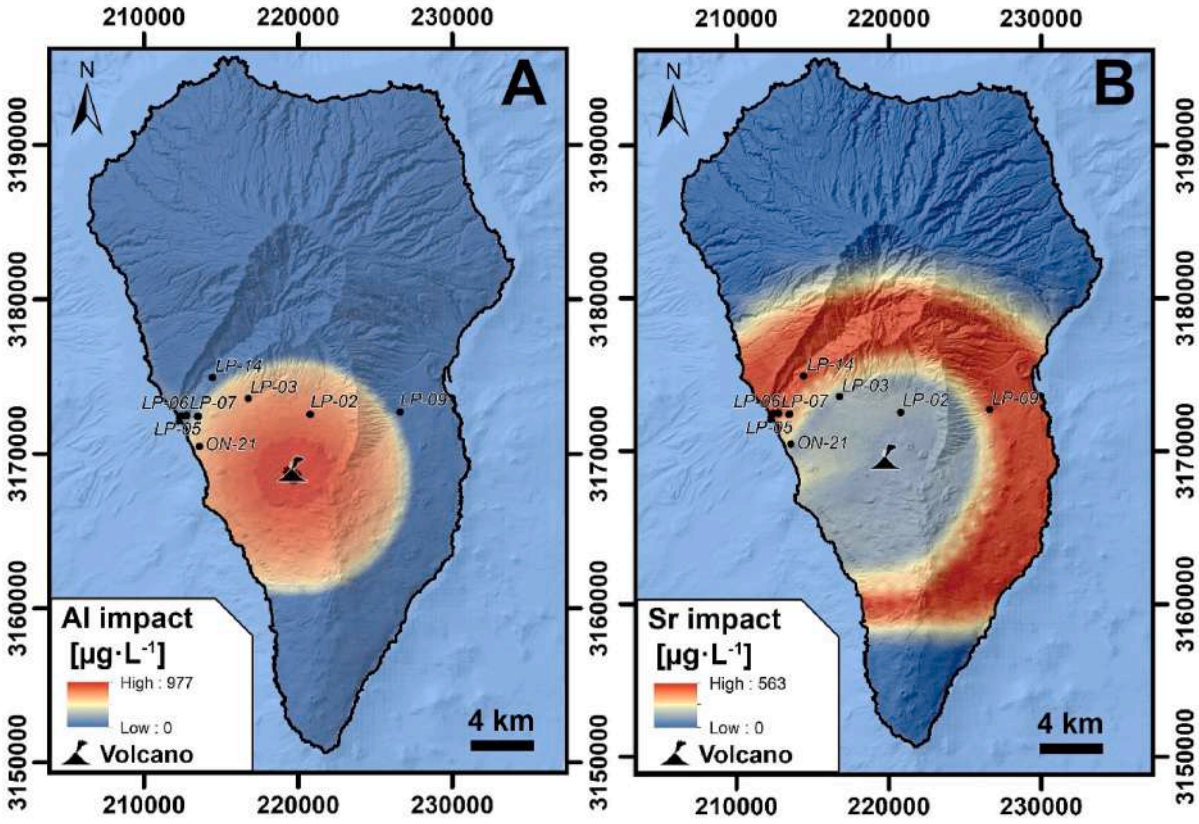

Fig. 5. Spatial distribution of hydrogeochemical impacts for Al (A) and Sr (B) with respect to distance to the volcano.

progressively decreasing once the eruption occurred (Fig. 7). Months after the eruption stopped, temperatures recovered, although not up to pre-eruption values. This could be interpreted as enhancement of the recharge introducing more fresh water into the insular aquifer system, with an increase of the vertical hydraulic conductivity favoring percolation or interconnectivity between perched groundwater bodies and the main regional aquifer of the island. However, LP-14 and LP-15, which are some of the closest sampling points to the volcano cone, reached 27.6 °C during eruption, and 25.2 °C post-eruption, respectively. This could entail that, for a certain proximity to the volcano, the heating effect of the eruption is higher than the cooling derived from the freshwater infiltration to the aquifers. Furthermore, this could also mean that in the areas furthest from the volcano, the thermal impact of the volcano has not yet ocurred. This situation is consistent with the typical significant retard thermal front of the advective heat transport within aquifers aquifer compared to the water flow (García-Gil et al., 2014). pH variations were also highly significant ($p < 0.0001$), with values dropping at eruption and slightly recovering after the eruption ended, but not reaching pre-eruption levels (Fig. 7), thus indicating substantial fluctuations in the acidity of the water. This is consistent with the CO_2 input from the volcanic gasses into groundwater, which would dissolve and lead to a significant drop in the pH values during the eruption. pH would be neutralizing slowly through water-rock interaction or new freshwater recharge, which would explain that pH values did not recover up to pre-eruption levels. Further assessment quantifying the CO_2 input will be performed through geochemical modelling in the next paper related to the present work, confirming that CO_2 input is the main process during the eruption that produces the pH drop in several sampling points. The redox potential (Eh mv) exhibited a highly significant difference ($p < 0.0001$) between eruption and post-eruption phases (Fig. 7), suggesting notable changes in the oxidation-reduction potential during different eruption times. This can be explained by the increased vertical permeability by fracture reactivations and new freshwater with higher oxidizing character infiltrating to the insular aquifer, as well as due to the mixing between the groundwater and deep hydrothermal fluids. Conductivity means for the different eruption phases did not show significant differences, but a tendency to slightly decrease during the eruption was observed, also consistent with the enhanced freshwater infiltration, as previously mentioned (Fig. 7).

Regarding the major ions studied (Fig. 7), most of them showed a slight to moderate concentration decrease during eruption, followed by a post-eruption recovery, but these differences were not statistically significant. A slight tendency towards statistical significance was found for sulfate (SO_4) levels ($p = 0.05$), which could be related to the differential input of $SO_2(g)$ from volcanic gasses or SO_4 dissolved in hydrothermal fluids.

However, more statistically significant differences were found among trace elements (Fig. 8). Most of them showed either an inverted "v" (Al, Cr, Fe, Mo, Ni, Sr, Th, Tl, V and Zn) or an increasing tendency (Ba, Cd, Co, Cu, Pb and U) among eruption phases, so that levels of the specific minor trace element increased during the eruption and then reverted to pre-eruption levels, or increased continuously due to the eruption, respectively. Finally, a few trace elements showed a decreasing tendency (As and Sb) or maintained relatively stable concentration levels (Ag, Be and Se) along the different eruption phases. Statistically significant differences were found for Al ($p = 0.042$) and Fe ($p = 0.02$); high statistical significances were detected for Ba, Cd and Tl ($p < 0.001$); and very high statistical significances were found for As, Pb, Sb, Th, and U. Zn concentration levels exhibited a tendency towards significance ($p = 0.051$). The trace elements displaying an inverted "V" undergo an instantaneous increase during the eruption, which is dissipated afterwards. This suggests an exogenous short-term process control due to the intermittent character of the increment, such as a possible effect of the rain and the volcanic ash leachates that would transport these trace elements during the infiltration into the groundwater. This effect would dilute after the volcano stops releasing ashes and after the

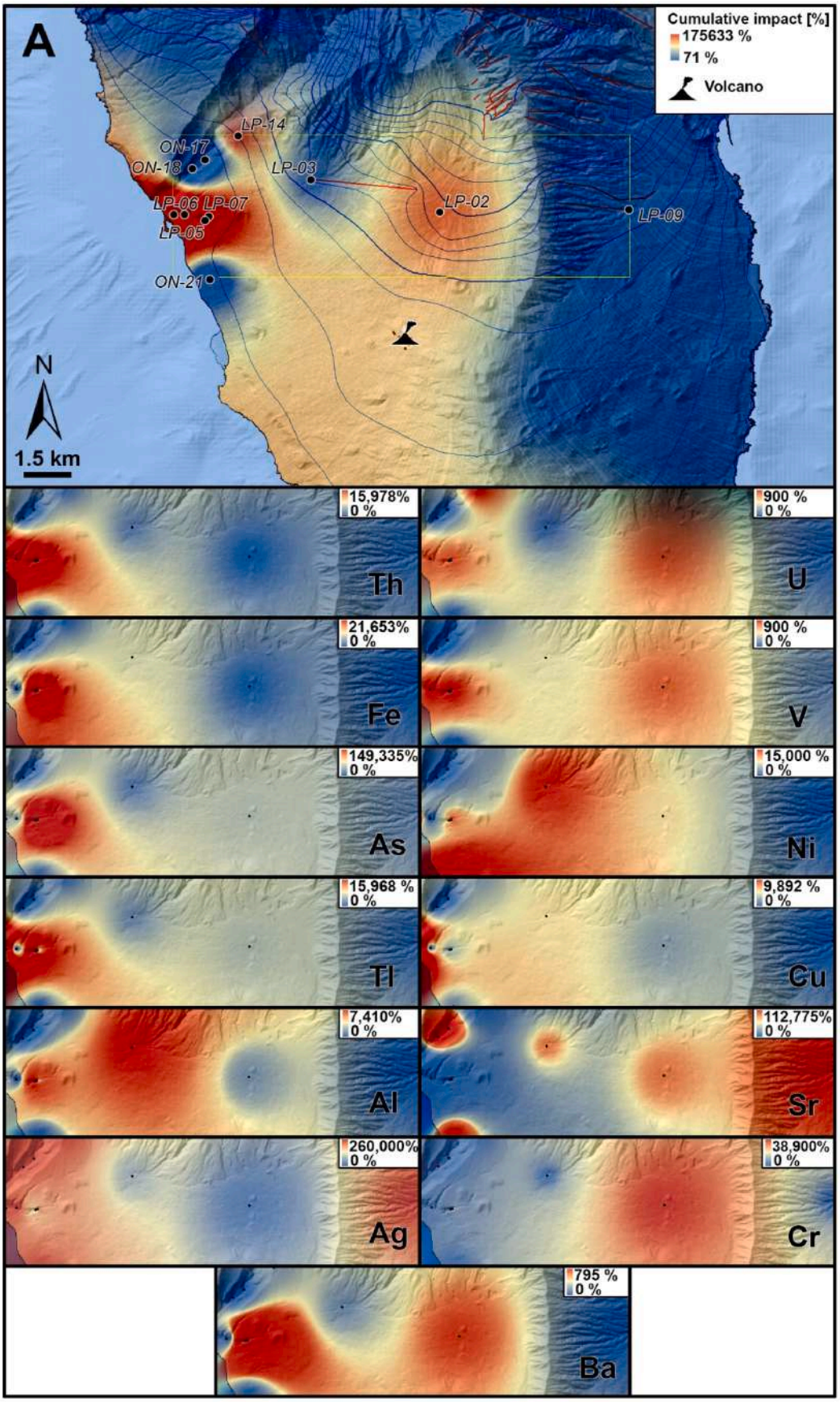

Fig. 6. Spatial distribution of hydrogeochemical impacts as cumulative impact at each monitored point (A) and for each trace metal investigated as percentage (%).

Table 4
Kruskall-Wallis test results for dependent variables during eruption time where statistical significance was found for $p < 0.05$. The table shows the Chi-Square test statistic, degrees of freedom (df), and the statistical significance (p) for each parameter. Statistical significance levels for $p < 0.0001$ (*), for $p < 0.001$ (**), and for $p < 0.05$ (^) are given.

Dependent variables	Chi-quare	df	Statistical Significance (p)
Temperature	10.241	2	0.006 **
pH	29.729	2	<0.0001 ***
Eh mv	63.792	2	<0.0001 ***
SO4	6.002	2	0.05 ^
Al	6.346	2	0.042
As	18.571	2	<0.0001 ***
Ba	13.923	2	0.001 **
Cd	14.827	2	0.001 **
Fe	7.806	2	0.02 *
Pb	35.045	2	<0.0001 ***
Sb	20.551	2	<0.0001 ***
Th	23.113	2	<0.0001 ***
Tl	14.370	2	0.001 **
U	21.136	2	<0.0001 ***
Zn	5.943	2	0.051 ^

existing ashes are leached by rainwater. On the other hand, the elements increasing constantly through the eruption stages and then not recovering to pre-existing values are more consistent to an endogenous control, since the deep hydrothermal flow and mixing with the groundwater, as well as the diffuse CO_2 input and the water-rock interactions, are processes taking place at longer time scales and at a more constant rate with respect to the rainwater and ash leachates recharge. Further, the groundwater mixing with volcanic ash leachates, deep hydrothermal fluids and CO_2 input will be modelled in the next paper of the series of three papers that constitute this comprehensive study.

These findings suggest that volcanic eruptions can have an important impact on the chemical composition of the water, thus emphasizing the need for careful monitoring and understanding of these changes to ensure effective management and protection of water resources in volcanic regions.

5.2.2. *Univariate analysis of the effect of the sample location on the studied parameters*

Concentration means were also compared in terms of the different sampling locations, using the same non-parametric statistical test, as part of the univariate analysis. All but six of the parameters studied (from a total of 39), showed statistically significant differences in their means among the different locations, so this independent variable exhibited a big importance, in addition to the eruption influence itself (Fig. 9). Most of the general parameters, major ions and trace elements showed a very high statistical significance ($p < 0.0001$), while five of them had high statistical significances (pH, Eh mv, Al, Be and Mn), three showed statistical significance below 0.005 (Pb – $p = 0.02$, Th – $p = 0.041$, and V – $p = 0.037$) and one showed tendency to significance (U, $p = 0.073$) (Table 5). A comprehensive table describing all the specific multiple comparisons is shown in Table S2.

LP-15, which is very close to the volcano cone was the one more frequently showing the highest values (15 of the total parameters analyzed), while LP-09 led the lowest values trend (8 of the total parameters studied). Interestingly, pH reached the lowest value at LP-15 (6.38), so acidification at this location was maximum due to the eruption, compared to other sampling points. Meanwhile, pH reached the most basic state at ON-17 (8.4), though this sampling point repeatedly reported a basic pH along the eruption phases. This entails that the volcanic CO_2 input that leads to significant drops in the pH values of groundwater would be released preferentially through the closest area to the volcanic cone, rather than through a completely diffuse input along the island groundwater. Conductivity heavily increased at this sampling point too, thus potentially changing the redox conditions radically for a certain period of time. Temperature reported the lowest values at LP-09 (16 °C) which, following the hypothesis of the enhanced freshwater recharge due to fracture reactivation, would entail that this sampling point was strongly affected by recharge. With regard to major ions, Ca, SO_4, HCO_3 and SiO_2 mean concentration levels where at their highest at LP-15, with very dramatic differences compared to the rest of sampling points. Since volcanic CO_2 dissolution leads to the increase in HCO_3 in the groundwater solutions, the observed increases at LP-15 in SO_4 (with origin likely in volcanic SO_2 input), HCO_3 and Ca (as rock-formin-element increased by enhanced acidity and rock dissolution) contents is consistent with the lowest pH value measured at this point, close to the volcanic cone, which would have undergone a high input of volcanic gases. No specific location showed a consistent low value among the major ions. Finally, trace elements showed a similar trend, where Ag, B, Ba, Be, Cd, Co, Cu, Fe, Hg, Mn, Ni and PB showed very different and elevated concentration means at LP-15 compared to all the other sampling points. With regard to the lowest values, they were mostly provided by LP-03 and LP-09 sampling points, coinciding with higher pH values and suggesting, thereby, a lower incidence of the volcanic gases input to these groundwater, as well as a lower incidence of other mentioned volcanic related processes, such as the ash-leachate infiltration. This would be consistent with the fact that LP-03 and LP-09 are water galleries that reach the Seamount Series, a less permeable unit with respect to the rest of the sampling points, which would explain that these points are less affected by the hydrochemical processes related to volcanic activity, which show higher incidence in the upper permeable units.

5.2.3. *Multivariate analysis of sample location and eruption phase on the parameters studied*

In addition to performing a comprehensive univariate analysis, a multivariate statistical analysis via MANOVA was performed to determine the potential impact of the combined effect of both independent variables (sample location and eruption phase) on the target dependent variables.

A main effect of eruption phase was found $F(6, 108) = 3.93$, $p = 0.001$; Wilks' $\Lambda = 0.674$; $\eta p^2 = 0.179$), showing that the changes in the physico-chemical parameters (pH, conductivity, redox potential and temperature) for some locations were bigger than for others. A main effect of location was also found $F(48, 161.403) = 11.912$, $p < 0.0001$; Wilks' $\Lambda = 0.011$; $\eta p^2 = 0.777$), with an even higher statistical significance. There was no significant main effect of the eruption phase and location interaction $F(48, 161.403) = 0.955$, $p = 0.561$; Wilks' $\Lambda = 0.475$; $\eta p^2 = 0.220$). Thus, a direct relationship between the four dependent variables, together with the combined effect of the two independent variables was not found, meaning that the changes in the parameter values due to the eruption phase were not influenced by location. However, as aforementioned, significant association between each of the independent variables and temperature, pH and conductivity alone were found and thoroughly described in the univariate analysis.

A statistically very significant main effect of eruption phase and location interaction on the concentrations of all the major ions combined was found ($F(77, 97.329) = 4.397$, $p < 0.0001$; Wilks' $\Lambda = 0.000$; $\eta p^2 = 0.723$). Remarkably, Wilks' Λ got a 0.000 value, which means that there is no variance which is unexplained by the independent variables, *i.e.*, most probably the changes in major ions concentrations are mostly due to the location of the measurement and the eruption. This can be related to the effect of the mentioned volcanic processes, as enhanced hydrothermal fluids or volcanic gases input to groundwater would take place with higher incidence at certain locations with higher proximity to the volcanic eruption, among other possible related and complex factors, such as differential permeabilities or flow regimes of the locations, that will be further assessed in the next works. Main effects of eruption phase ($F(22, 30) = 9.059$, $p < 0.0001$; Wilks' $\Lambda = 0.017$; $\eta p^2 = 0.869$) and location ($F(88, 107.821) = 36.147$, $p < 0.0001$; Wilks' $\Lambda = 0.000$; $\eta p^2 = 0.939$) were also found. Simple main effects analysis showed that the sample location had a statistically significant effect on most of the major

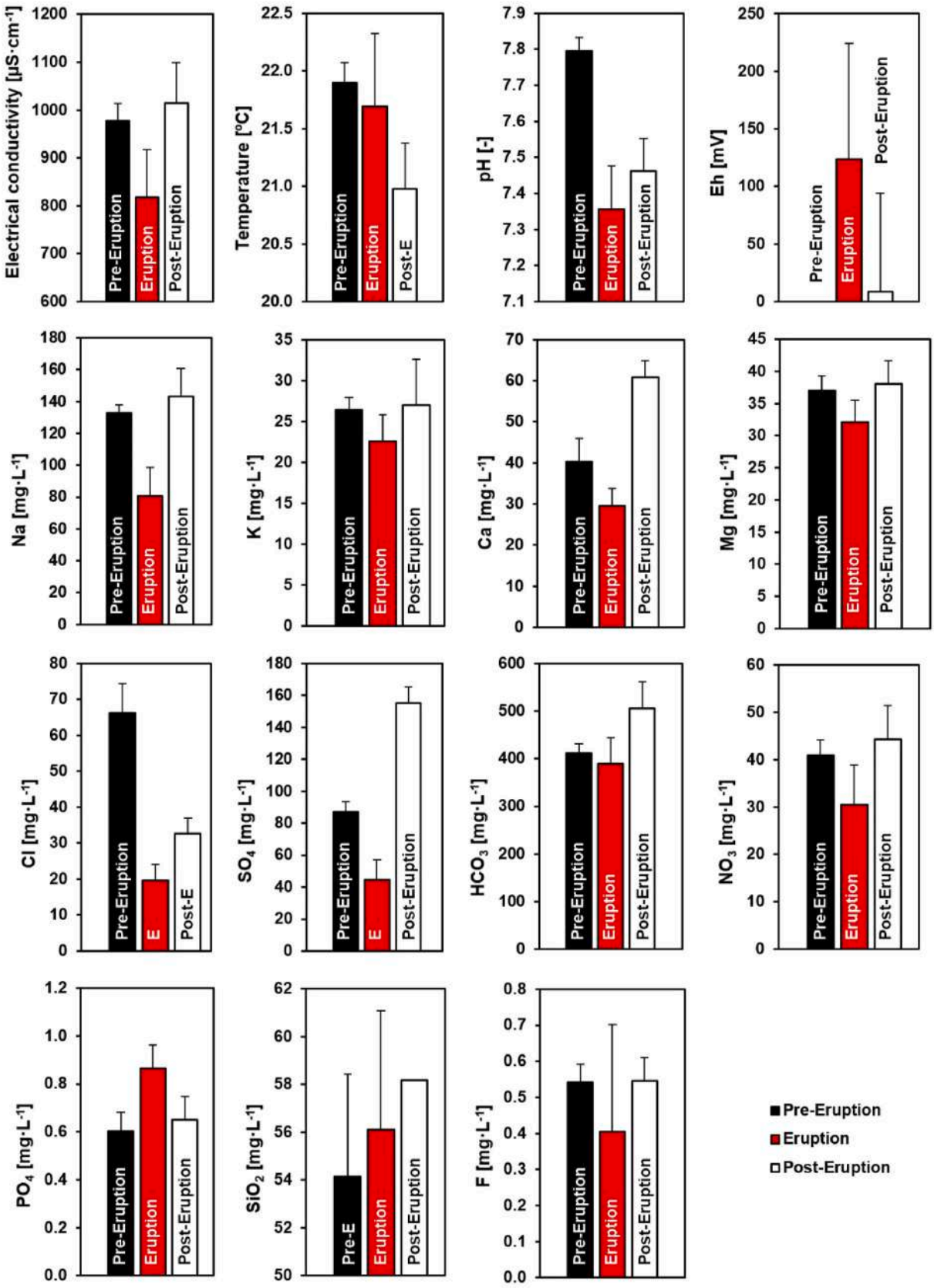

Fig. 7. Comparison of mean differences ± SEM for physico-chemical parameters, minor and major elements among the three distinct eruption phases: pre-eruption, eruption, and post-eruption.

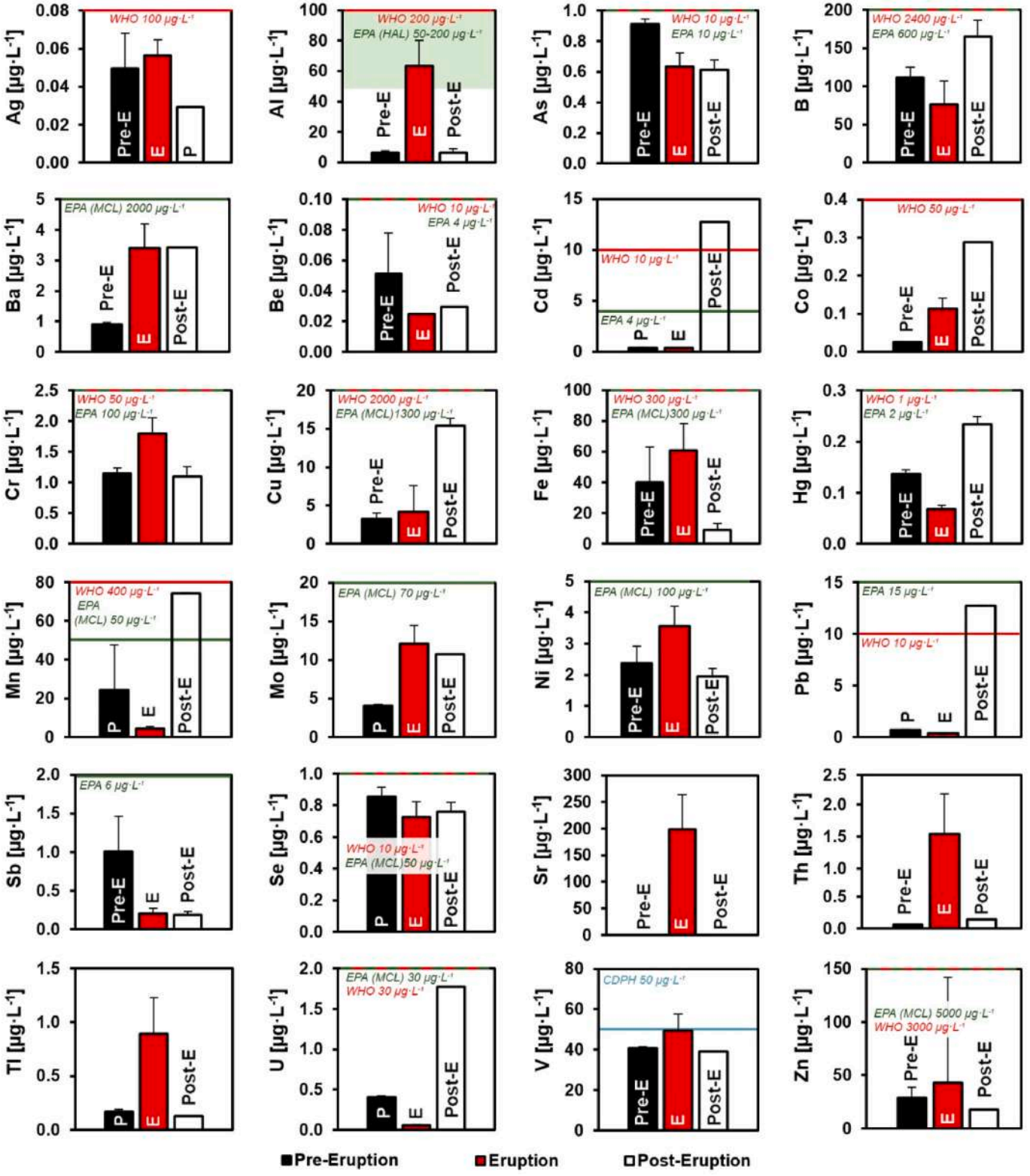

Fig. 8. Comparison of mean differences ± SEM in trace elements among three distinct eruption phases: pre-eruption, eruption, and post-eruption. Drinking water quality standards are displayed (EPA, 2001; EPA, 2009; WHO, 2004; WHO, 2011).

ions but F, while eruption had a statistically significant effect on less of them. Thus, the closeness or farness of the sample to the volcano seemed to be more important. It is worth highlighting the affectation of both independent variables on F, Na and SO_4, when also observing the F values, p and Partial Eta Squared Values together. Tukey post hoc tests were performed after assessing the general results for the multivariate analysis. This test indicated that the eruption caused the concentration levels to be statistically different for all the major ions studied, with except of PO_4, for both pre-eruption and eruption means, and for most of major ions for eruption and post eruption means (Table S3). The specific mean differences between sample locations could not be assessed using Tukey in the multivariate analysis due to some of the locations having a

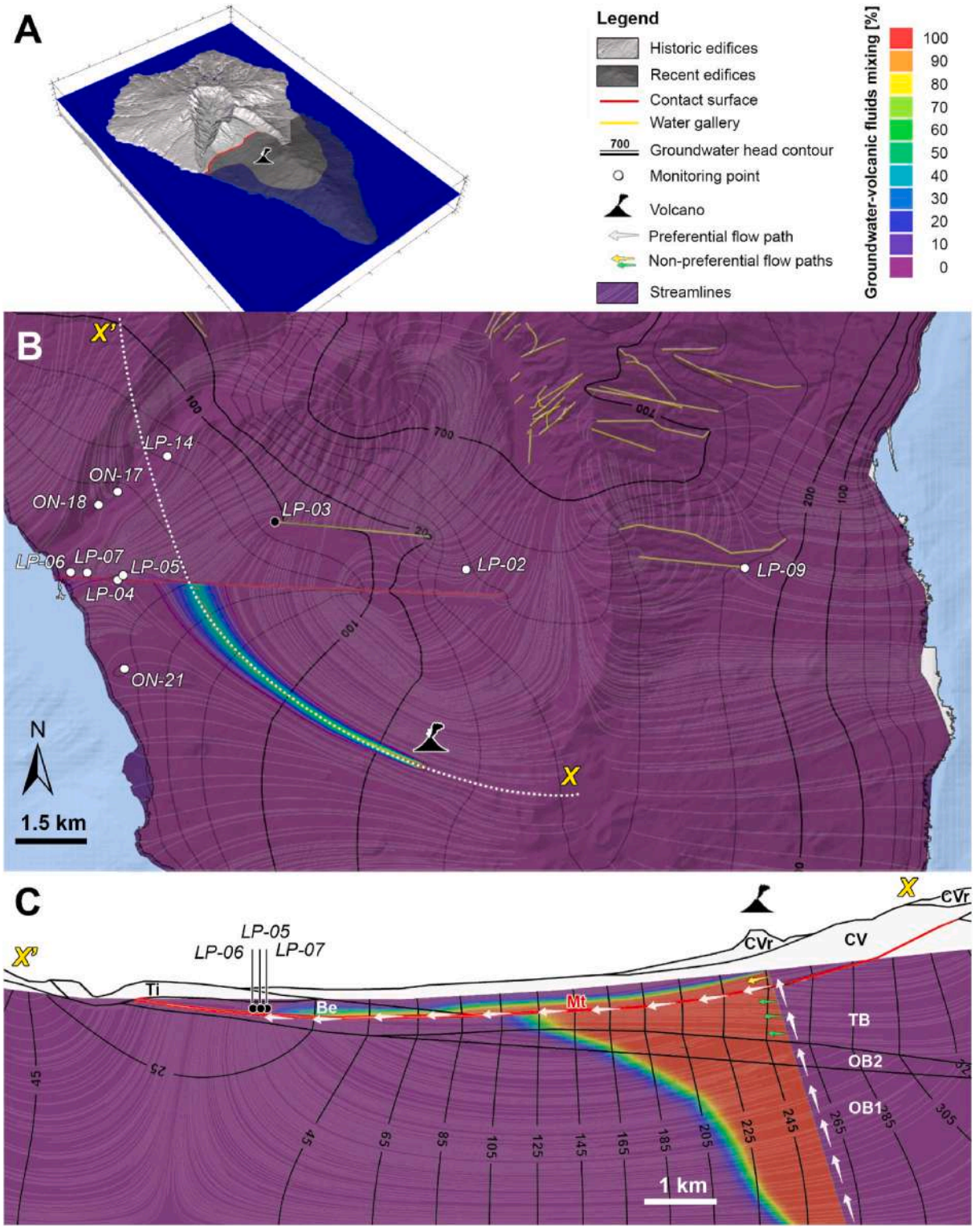

Fig. 9. 3D diagram of *La Palma* Island illustrating the contact surface between historic (pre-*Tajogaite*) and recent volcanic edifices (A). Head contour map illustrating the potential groundwater-volcanic fluid mixing plume originating from the investigated volcano area towards LP-05-07 wells (B), and xx' vertical cross-section displaying the vertical geological discretization and potential preferential flow paths (C). The submarine edifice (OB1, OB2), *Taburiente* edifice (TB), *Bejenado* edifice (Be), *Time* sedimentary materials (Ti), *Tajogaite* edifice (CV), and recent *Tajogaite* eruptions (CVr) are depicted.

very small sample size. These differences were, nonetheless, studied in the univariate analysis described in the previous section.

Multivariate statistical analysis could not be performed for minor ions due to the sample being too small for some of the groups or the data variance being too small. However, an extensive univariate statistical analysis was performed.

The marginal means obtained from the multivariate statistical analysis indicated that, for most of the parameters studied, their observed values at the different locations depended on the joint impact of the sample location and whether the eruption was active or not. This

Table 5
Kruskall-Wallis test results for the univariate analysis comparing sampling location means. The table shows the Chi-Square test statistic, degrees of freedom (df), and the statistical significance (p) for each parameter. Statistical significance was set at $p < 0.05$, high significance at $p < 0.001$ (**) and very high significance at $p < 0.0001$ (*).

Parameter	Chi-Square	df	Statistical Significance (p)
Conductivity	110.391	15	<0.0001 ***
Temperature	40.747	15	<0.0001 ***
pH	32.08	15	0.006 **
Eh mv	32.113	15	0.006 **
Na	115.785	15	<0.0001 ***
K	120.918	15	<0.0001 ***
Ca	86.08	15	<0.0001 ***
Mg	90.583	15	<0.0001 ***
Cl	123.892	15	<0.0001 ***
SO4	111.546	15	<0.0001 ***
HCO3	101.654	15	<0.0001 ***
NO3	96.711	15	<0.0001 ***
PO4	75.056	15	<0.0001 ***
SiO2	44.365	7	<0.0001 ***
F	84.136	15	<0.0001 ***
Conductivity at 20°C	99.349	15	<0.0001 ***
Al	36.626	15	0.001 **
As	54.939	15	<0.0001 ***
Ba	34.491	7	<0.0001 ***
Be	20.05	7	0.005 **
Cd	57.737	15	<0.0001 ***
Cr	45.553	15	<0.0001 ***
Cu	40.792	15	<0.0001 ***
Fe	55.407	15	<0.0001 ***
Hg	47.146	15	<0.0001 ***
Mn	33.357	15	0.004 **
Mo	35.719	7	<0.0001 ***
Ni	44.414	15	<0.0001 ***
Pb	28.34	15	0.02 *
Sb	49.113	15	<0.0001 ***
Se	70.211	15	<0.0001 ***
Th	14.66	7	0.041 *
U	12.962	7	0.073 ^
V	13.999	6	0.037 *

was represented by the distance found between the three categories of the eruption independent variable. Those locations where the categories were overlapping indicated that all the variance in the parameter values is explained by location and eruption phase, while those where a separation between lines is observed, indicated that some other variables must be influencing the parameter values. Interestingly, the latter was the case for LP-15 (Fig. S6). This sampling point corresponded to a water spring, where different variables seem to have an important enough effect on parameter values so that some of the variance found in the parameters is not explained by the eruption. LP-15 (Naciente dos aguas) is a thermal spring that shows very high HCO_3 (1660 mg/L) and SiO2 (119.6 mg/L) concentrations, which implies a high connection and proportion of deep hydrothermal fluids, with high temperatures and CO2 pressures at depth. Thereby, this higher connection with deep hydrothermal fluids in LP-15 is consistent with the fact that some of its variance is not explained by the independent variables studied, since the hydrochemical parameters would be mainly controlled by the proportion of hydrothermal fluids input to this sampling point. However, the deep hydrothermal character (high HCO_3 and SiO_2) of LP-15 is enhanced in the post-eruption stage, which means there could be a possible relation between the eruption and the increased ascent of hydrothermal fluids with a certain delay after the eruption. This process will be further investigated and modelled in the next works of this series of articles.

5.3. Hydrogeological and hydrochemical conceptual model for the 2021 La Palma volcanic eruption

The univariate and multivariate statistical analysis results described in the previous sections indicated that there were significant effects related to the volcanic activity associated to the 2021 La Palma eruption that led to the hydrochemical changes measured in several of the dependent variables for most of the samples, mainly on T, pH, HCO_3, conductivity, as well as high increases in several trace element concentrations and drops in some of the major ions such as Na, Ca, SO_4 and F. T and pH also show dropped in the eruption stage. The majority of the studied parameters correlate with the eruption stage and the location of the sample, although a higher number of parameters show high significance in the correlation with location compared to with eruption stage. Thus, the closeness or farness of the sample to the volcano seemed to be the most important factor.

Concentrations of Al, Cr, Fe, Mo, Ni, Sr, Th, Tl, V and Zn in groundwater showed an instant increase peak during the eruption, that is diluted in the post-eruption stage and that, thereby, can be attributed to an exogenous intermittent control that it is likely related to the infiltration of volcanic ash leachates. In addition, the chemical analysis of volcanic ash leachates showed very high concentrations of this group of elements, mainly regarding Al (up to 3.17 mg/L), with concentrations much higher than those found in any other groundwater of the island, which supports the explanation of the volcanic ash leachates infiltration. On the other hand, Ba, Cd, Co, Cu, Pb and U, showed a constant increase tendency leading to concentrations that are maintained in the post-eruption stage, which can attributed to an endogenous control by long-term and constant effects of processes as additional input of deep hydrothermal fluids to the aquifers. Further, the thermal water analysis performed in similar basaltic-hosted geothermal systems in Iceland (e.g. Kaasalainen et al., 2015), that represent the pure deep hydrothermal end member of this type of waters, show high concentrations in the last mentioned group of trace elements and in similar proportions, which supports the explanation of an additional input of deep hydrothermal fluids to the freshwater aquifers in La Palma as a consequence of the volcanic eruption.

As a summary, the variance measured in the groundwater hydrochemistry of La Palma throughout the different eruption stages would be mainly controlled by the following hydrogeochemical and volcanic processes: 1) Enhanced freshwater recharge (rainwater or lower T groundwater infiltration to deeper aquifers) by fracture reactivation due to volcanic activity (Fig. 9); 2) Volcanic CO_2(g) input dissolved in groundwater, preferentially affecting the areas close to the volcano; 3) Deep hydrothermal water input to freshwater aquifers, leading to the increase in SiO2, several major elements such as Na, Ca and SO4, and specially in several minor and trace elements as Ba, Cd, Co, Cu, Pb and U. The sampling point LP-15, with a chemical composition consisting of high concentrations of SiO_2 and HCO_3, which characterizes the deep hydrothermal fluids in these basaltic hosting rocks, is the sample that represents the higher incidence of this hydrothermal water and, thereby, the higher connection with the deep geothermal system of the island; 4) Volcanic ash leachates infiltration into groundwater, leading to the instant increase during the eruption in the concentrations of Al, Cr, Fe, Mo, Ni, Sr, Th, Tl, V and Zn.

6. Conclusions

A statistical study of the impacts of the Tajogaite 2021 eruption in *La Palma* on the hydrochemical parameters of the groundwater was performed, applied to 35 water samples in 15 different sampling points at pre-eruption, eruption and post-eruption stages. The means for the different parameters studied through the different eruption stages were compared using Kolmogorov-Smirnov and Levene's test, Mann–Whitney and Kruskall-Wallis plus post-hoc test. A multivariate two-way MANOVA test was performed to determine the combined impact of the independent variables (geographical location and eruption stage) on the dependent variables.

The univariate and multivariate statistical analysis results indicate that there are very significant effects related to the volcanic activity that

led to the hydrochemical changes observed in several of the dependent variables in most of the samples, mainly in T, pH, HCO_3, conductivity, some major ions as Na, Ca, SO_4 and F, and mostly in several trace element concentrations.

The univariate analysis showed that most of the studied hydrochemical parameters correlate significantly with both the eruption stage and the location of the sample, although a higher number of parameters show high significance in the correlation with location compared to eruption stage. Thus, the closeness or farness of the sample to the volcano seemed to be more important. Further, the multivariate analysis carried out in order to assess the influence of the combined effect of the two independent variables on the hydrochemical parameters indicate that no statistical significance is obtained for the correlation between those parameters and the eruption stage and location together. This means that the eruption changes are mainly controlled by the location of the measurement and whether the eruption was active or not.

The minor and trace elements were the parameters that showed the highest variation due to the eruption effect, although different behavior patterns were observed. There is a group of elements constituted by Al, Cr, Fe, Mo, Ni, Sr, Th, Tl, V and Zn that showed an instant increase peak during the eruption, which gets diluted in the post-eruption stage and that, thereby, could be attributed to an exogenous intermittent control related to the infiltration of volcanic ash leachates. Another group of elements constituted by Ba, Cd, Co, Cu, Pb and U, showed a constant increase tendency leading to concentrations that are maintained in the post-eruption stage, which have been attributed to an endogenous control by long-term and constant effects of processes as additional input of deep hydrothermal fluids to the aquifers, since other examples of thermal waters hosted in basalts worldwide show high concentrations in those trace elements.

Finally the analysis of the marginal means indicated that, for most of the samples, all the variance in the parameter values is explained by location and eruption phase, while for one exception represented by the sampling point LP-15 other variables must be influencing the parameter values. This sampling point corresponded to a thermal water spring, where different variables would have an important effect on hydrochemical parameters, since some of the variance found in the parameters is not explained by the eruption. This is due to the fact that this spring, with very high concentrations of SiO_2 and HCO_3, has a chemical composition that characterizes the deep hydrothermal fluids. Thus, this spring would be affected by the input of different amounts of the ascending deep fluid, enhanced during and after the eruption and leading to the increase in SiO_2 and HCO_3, among other elements. This spring and this hydrothermal process, together with the other thermal spring in the island (Fuente Santa), would have a high relevance to characterize the deep hydrothermal end member of the geothermal system in La Palma island.

Summarizing the main outcomes of the statistical analysis results, it can be interpreted that the variance measured in the groundwater hydrochemistry for La Palma throughout the different eruption stages would be mainly controlled by the location of the sample (distance to the volcanic cone) and whether the eruption was active or not. Besides, different potential hydrogeochemical and volcanic processes could be controlling the measured variability. The enhanced freshwater recharge by fracture reactivation due to volcanic activity is traduced into instant drops of T and conductivity, generally almost recovered post-eruption. Next, a volcanic CO_2(g) input dissolved in groundwater could be leading to the significant measured drops in pH and increments in HCO_3, which could be traduced in an increased reactivity with the hosting rocks, and that would preferentially affect the sampling points close to the volcanic eruption. Another important process involved in the system would be the deep hydrothermal water input to the freshwater aquifers, leading to the increase in SiO_2, and several major and minor and trace elements, with a higher incidence in the deeper sampling points, such as the galleries at LP-03 and LP-09, or the thermal spring LP-15. However, a difuse affectation was also observed on several points in the island. Finally, the volcanic ash leachates infiltration into groundwater would be related to the instant increase during the eruption in the concentrations of Al, Cr, Fe, Mo, Ni, Sr, Th, Tl, V and Zn. This process affects with a higher incidence in the samples gathered in the central West coastline of the island, which could be acting as a hydrological collecting point of the rainwater and groundwater flow (see Fig. 9B). Further, this conceptual model and the origin of the hydrogeochemical effects will be contrasted by quantifying these processes through coupled hydrological and geochemical modelling in the next articles.

The variations in trace element concentrations provide valuable insights into the behavior of these elements during volcanic eruptions and their interaction with groundwater. The findings of this work emphasize the significance of continuous monitoring and assessment of trace element concentrations in groundwater, both prior to and following volcanic events, in order to comprehensively comprehend their environmental consequences and potential hazards to human and ecological well-being. Additionally, it is worth noting that fluctuations in water chemistry have played a pivotal role in evaluating volcanic hazards. Notably, pertinent chemical alterations have been promptly reported to national-level institutions involved in disaster prevention, as well as to scientific committees responsible for volcano-prone regions. The integrated data obtained from monitoring systems have been instrumental in making informed decisions aimed at safeguarding the population.

Declaration of competing interest

The authors declare that they have no known competing financial interests or personal relationships that could have appeared to influence the work reported in this paper.

Data availability

Data will be made available on request.

7. Acknowledgements

This research was supported by the European Union's Horizon 2020 Research and Innovation Program (project ARSINOE 101037424). This research was partially supported by the Spanish Research Agency (project SAGE4CAN PID 2020-114218RA-100). Authors are grateful to the *Consejo Insular de Aguas de La Palma* (*CIALP*), insular Water Authority, for the valuable support.

Appendix A. Supplementary data

Supplementary data to this article can be found online at https://doi.org/10.1016/j.gsd.2023.100992.

References

Allard, P., Jean-Baptiste, P., D'Alessandro, W., Parello, F., Parisi, B., Flehoc, C., 1997. Mantle-derived helium and carbon in groundwaters and gases of Mount Etna, Italy. Earth Planet Sci. Lett. 148, 501–516.

Ancochea, E., Hernán, F., Cendrero, A., Cantagrel, J.M., Fúster, J., Ibarrola, E., et al., 1994. Constructive and destructive episodes in the building of a young oceanic island, La Palma, canary islands, and genesis of the caldera de Taburiente. J. Volcanol. Geoth. Res. 60, 243–262.

APHP, 1992. Avance del Plan Hidrológico de La Palma. Cabildo Insular de La Palma, Santa Cruz de Tenerife, p. 245.

Appelo, C.A.J., Postma, D., 2005. Geochemistry, Groundwater and Pollution, second ed. CRC Press.

APPHLP, 2012. Avance o Proyecto del Plan Hidrológico de Palma. Memoria de Información. Consejo Insular de Aguas de La Palma, La Palma, p. 136.

Armienta, M.A., De la Cruz-Reyna, S., 1995. Some hydro-geochemical fluctuations observed in Mexico related to volcanic activity. Appl. Geochem. 10, 215–227.

Armienta, M.A., De la Cruz-Reyna, S., Gómez, A., Ramos, E., Ceniceros, N., Cruz, O., et al., 2008. Hydrogeochemical indicators of the Popocatépetl volcano activity. J. Volcanol. Geoth. Res. 170, 35–50.

Aubaud, C., Athanase, J.-E., Clouard, V., Barras, A.-V., Sedan, O., 2013. A review of historical lahars, floods, and landslides in the Prêcheur river catchment (Montagne Pelée volcano, Martinique island, Lesser Antilles). Bull. Soc. Geol. Fr. 184, 137–154.

Auge, M., Viale, G., Sierra, L., 2013. Arsénico en el agua subterránea de la Provincia de Buenos Aires.
Barberi, F., Bertagnini, A., Landi, P., Principe, C., 1992. A review on phreatic eruptions and their precursors. J. Volcanol. Geoth. Res. 52, 231–246.
Bhattacharya, P., Claesson, M., Bundschuh, J., Sracek, O., Fagerberg, J., Jacks, G., et al., 2006. Distribution and mobility of arsenic in the Río Dulce alluvial aquifers in Santiago del Estero Province, Argentina. Sci. Total Environ. 358, 97–120.
Casadevall, T., de la Cruz, S., Rose, W., Bagley, S., Finnegan, D., Zoller, W., 1984. Volcán El Chichón México: the crater lake and thermal activity. J. Volcanol. Geoth. Res. 23, 169–191.
Custodio, E., 2020. Hydrogeology and Groundwater Resources in Volcanic Formations and Islands. Universidad Politécnica de Cataluña, Barcelona.
Custodio, E., Cabrera, MdC., Poncela, R., Puga, L.-O., Skupien, E., del Villar, A., 2016. Groundwater intensive exploitation and mining in Gran Canaria and Tenerife, Canary Islands, Spain: hydrogeological, environmental, economic and social aspects. Sci. Total Environ. 557–558, 425–437.
de Hoog, J.C.M., Koetsier, G.W., Bronto, S., Sriwana, T., van Bergen, M.J., 2001. Sulfur and chlorine degassing from primitive arc magmas: temporal changes during the 1982–1983 eruptions of Galunggung (West Java, Indonesia). J. Volcanol. Geoth. Res. 108, 55–83.
De la Cruz-Reyna, S., Armienta, M., Zamora, V., Juárez, F., 1989. Chemical changes in spring waters at Tacaná volcano, Chiapas, Mexico: a possible precursor of the May 1986 seismic crisis and phreatic explosion. J. Volcanol. Geoth. Res. 38, 345–353.
De la Cruz-Reyna, S., Tilling, R.I., 2008. Scientific and public responses to the ongoing volcanic crisis at Popocatépetl Volcano, Mexico: importance of an effective hazards-warning system. J. Volcanol. Geoth. Res. 170, 121–134.
De la Nuez, J., Casillas, R., Martín, M.C., 2008. In: Cabrera, PTy (Ed.), Estructura interna y vulcanismo reciente de la Isla de La Palma, vol. 4. Geoguías, pp. 127–153.
Delmelle, P., Gerin, P., Oskarsson, N., 2000. Surface and bulk studies of leached and unleached volcanic ashes. EOS, Transactions, American Geophysical Union 81, F1311.
Duncan, D., 2012. Freshwater under Threat: Pacific Islands. Vulnerability Assessment of Freshwater Resources to Environmental Change Regional Office for Asia and the Pacific. Bangkok, p. 66.
EGDHLP, 2009. Estudio General de la Demarcación Hidrográfica de La Palma. Plan Hidrológico. Consejo Insular de Aguas de La Palma, La Palma, p. 105.
EPA, 2001. Parameters of Water Quality - Interpretation and Standards. Environmental Protection Agency, Ireland, Ireland, p. 133.
EPA, 2009. National recommended water quality criteria. In: Water Oo. US Environmental Protection Agency, Washington D. C.
Federico, C., Aiuppa, A., Allard, P., Bellomo, S., Jean-Baptiste, P., Parello, F., et al., 2002. Magma-derived gas influx and water-rock interactions in the volcanic aquifer of Mt. Vesuvius, Italy. Geochem. Cosmochim. Acta 66, 963–981.
Fischer, T.P., Arellano, S., Carn, S., Aiuppa, A., Galle, B., Allard, P., et al., 2019. The emissions of CO2 and other volatiles from the world's subaerial volcanoes. Sci. Rep. 9, 18716.
García-Gil, A., Fontes, J.C., Santamarta, J.C., 2022. Groundwater conditions the effectiveness of surface water diversion in the remediation of the eutrophicated volcanic lake of Furnas, Azores archipelago. Sci. Total Environ. 837, 155789.
García-Gil, A., Jimenez, J., Marazuela, M.Á., Baquedano, C., Martínez-León, J., Cruz-Pérez, N., et al., 2023. Effects of the 2021 La Palma volcanic eruption on groundwater resources (Part I): hydraulic impacts. Groundwater for Sustainable Development 22, 114–125.
García-Gil, A., Vázquez-Suñe, E., Garrido, E., Sánchez-Navarro, J.A., Mateo-Lázaro, J., 2014. The Thermal Consequences of River-Level Variations in an Urban Groundwater Body Highly Affected by Groundwater Heat Pumps. Science of the Total Environment.
García, M.G., Lecomte, K.L., Stupar, Y., Formica, S.M., Barrionuevo, M., Vesco, M., et al., 2012. Geochemistry and health aspects of F-rich mountainous streams and groundwaters from sierras Pampeanas de Cordoba, Argentina. Environ. Earth Sci. 65, 535–545.
Garlick, G., Wedepohl, K., 1969. Handbook of Geochemistry.
Gasco-Cavero, S., García-Gil, A., Cruz-Pérez, N., Rodríguez, L.F.M., Laspidou, C., Contreras-Llin, A., et al., 2023. First emerging pollutants profile in groundwater of the volcanic active island of El Hierro (Canary Islands). Sci. Total Environ., 162204
Giammanco, S., Ottaviani, M., Valenza, M., Veschetti, E., Principio, E., Giammanco, G., et al., 1998. Major and trace elements geochemistry in the ground waters of a volcanic area: Mount Etna (Sicily, Italy). Water Res. 32, 19–30.
Giggenbach, W., 1996. Chemical Composition of Volcanic Gases. Monitoring and Mitigation of Volcano Hazard. Springer, Berlin, pp. 222–256.
Goff, F., Love, S.P., Warren, R., Counce, D., Obenholzner, J., Siebe, C., et al., 2001. Passive infrared remote sensing evidence for large, intermittent CO2 emissions at Popocatépetl volcano, Mexico. Chem. Geol. 177, 133–156.
Gomez, M., Blarasin, M., Martínez, D., 2009. Arsenic and fluoride in a loess aquifer in the central area of Argentina. Environ. Geol. 57, 143–155.
Guillou, H., Carracedo, J.C., Torrado, F.P., Badiola, E.R., 1996. K-Ar ages and magnetic stratigraphy of a hotspot-induced, fast grown oceanic island: El Hierro, Canary Islands. J. Volcanol. Geoth. Res. 73, 141–155.
Hayes, D.E., Rabinowitz, P.D., 1975. Mesozoic magnetic lineations and the magnetic quiet zone off northwest Africa. Earth Planet Sci. Lett. 28, 105–115.
Herd, R.A., Edmonds, M., Bass, V.A., 2005. Catastrophic lava dome failure at Soufrière Hills volcano, Montserrat, 12–13 July 2003. J. Volcanol. Geoth. Res. 148, 234–252.
Hiltona, D.R., Macphersona, C.G., Elliottb, T.R., 2000. Helium isotope ratios in mafic phenocrysts and geothermal fluids from La Palma, the Canary Islands (Spain): implications for HIMU mantle sources. Geochem. Cosmochim. Acta 64, 2119–2132.
Jasim, A., Hemmings, B., Mayer, K., Scheu, B., 2019. Groundwater Flow and Volcanic Unrest. From Science to Society, Volcanic Unrest, pp. 83–99.
Karakaya, M.Ç., Karakaya, N., Ş, Küpeli, Yavuz, F., 2012. Mineralogy and geochemical behavior of trace elements of hydrothermal alteration types in the volcanogenic massive sulfide deposits, NE Turkey. Ore Geol. Rev. 48, 197–224.
Kim, J.Y., Naboa, E.E., Amidon, F., Reeves, M.K., Miller, S.E., 2020. Hawaiian islands coastal ecosystems: past, present, and future. In: Goldstein, M.I., DellaSala, D.A. (Eds.), Encyclopedia of the World's Biomes. Elsevier, Oxford, pp. 157–174.
Kolomyts, E.G., 2019. Local evolutionary processes in the forest ecosystems of volcanic islands of the northwestern pacific. Geogr. Nat. Resour. 40, 63–73.
Kruse, E., Ainchil, J., 2003. Fluoride variations in groundwater of an area in buenos aires province, Argentina. Environ. Geol. 44, 86–89.
Lachowycz, S.M., Pyle, D.M., Mather, T.A., Varley, N.R., Odbert, H.M., Cole, P.D., et al., 2013. Long-range correlations identified in time-series of volcano seismicity during dome-forming eruptions using detrended fluctuation analysis. J. Volcanol. Geoth. Res. 264, 197–209.
Langmuir, D., 1997. Aqueous Environmental Geochemistry. Prentice Hall.
López-Saavedra, M., Martí, J., 2023. Reviewing the multi-hazard concept. Application to volcanic islands. Earth Sci. Rev. 236, 104286.
Mair, A., El-Kadi, A.I., 2013. Logistic regression modeling to assess groundwater vulnerability to contamination in Hawaii, USA. J. Contam. Hydrol. 153, 1–23.
Navarro Latorre, J.M., 1993. Mapa Geológico de La Palma. Ministerio de Agricultura, Pesca y Alimentación-ICONA, Madrid.
Nicolli, H.B., Suriano, J., Gomez Peral, M.A., Ferpozzi, L.H., Baleani, O.A., 1989. Groundwater contamination with arsenic and other trace elements in an area of the pampa, province of Córdoba, Argentina. Environ. Geol. Water Sci. 14, 3–16.
Padrón, L., Paz, S., Gutiérrez, A., Rubio, C., Weller, D., Torre, A., 2020. Metal Content and Trace Elements in Groundwater Supply of the Island of El Hierro (Canary Islands, Spain). Revista espanola de salud publica, p. 94.
Parello, F., Allard, P., D'Alessandro, W., Federico, C., Jean-Baptiste, P., Catani, O., 2000. Isotope geochemistry of Pantelleria volcanic fluids, Sicily Channel rift: a mantle volatile end-member for volcanism in southern Europe. Earth Planet Sci. Lett. 180, 325–339.
PEVOLCA, 2021. Scientific Committee Report 25/12/2021: Actualización de la actividad volcánica en Cumbre Vieja (La Palma).
Poncela, R., 2009. Definición del modelo conceptual del flujo subterráneo de la Isla de La Palma. Gobierno de Canarias, Santa Cruz de Tenerife, p. 144.
Poncela, R., 2015. La Palma Volcanic Aquifer System Hydrogeology Civil Engineering Department. Alicante University, Islas Canarias, p. 227.
Poncela, R., Santamarta, J.C., García-Gil, A., Cruz-Pérez, N., Skupien, E., García-Barba, J., 2022. Hydrogeological characterization of heterogeneous volcanic aquifers in the Canary Islands using recession analysis of deep water gallery discharge. J. Hydrol. 610, 127975.
Poncela, R., Skupien, E., 2013. Estado de las masas de agua subterránea de La Palma. Consejo Insular de Aguas de La Palma, p. 131.
Santamarta, J.C., Lario-Bascones, R.J., Rodríguez-Martín, J., Hernández-Gutiérrez, L.E., Poncela, R., 2014. Introduction to hydrology of volcanic islands. IERI Procedia 9, 135–140.
Scarpa, R., Tilling, R.I., Martini, M., 1996. Chemical characters of the gaseous phase in different stages of volcanism: precursors and volcanic activity. Monitoring and mitigation of volcano hazards 199–219.
Silva, A.C., Hernández, M.A.A., Taran, Y., Ruiz, J.C.G., 2000. Chemical precursors to the 1998-1999 eruption of Colima volcano, Mexico. Rev. Mex. Ciencias Geol. 17, 111–124.
Smedley, P.L., Kinniburgh, D.G., 2002. A review of the source, behaviour and distribution of arsenic in natural waters. Appl. Geochem. 17, 517–568.
Smedley, P.L., Nicolli, H.B., Macdonald, D.M.J., Barros, A.J., Tullio, J.O., 2002. Hydrogeochemistry of arsenic and other inorganic constituents in groundwaters from La Pampa, Argentina. Appl. Geochem. 17, 259–284.
Sorey, M., Kennedy, B., Evans, W., Farrar, C., Suemnicht, G., 1993. Helium isotope and gas discharge variations associated with crustal unrest in Long Valley Caldera, California, 1989–1992. J. Geophys. Res. Solid Earth 98, 15871–15889.
Tribble, G., 2008. Ground Water on Tropical Pacific Islands-Uunderstanding a Vital Resource, p. 35.
Varley, N., Armienta, M., 2001. The absence of diffuse degassing at Popocatépetl volcano, Mexico. Chem. Geol. 177, 157–173.
White, I., Falkland, T., 2010. Management of freshwater lenses on small Pacific islands. Hydrogeol. J. 18, 227–246.
WHO, 2004. Guidelines for Drinking Water Quality. World Health Organization, Geneva.
WHO, 2011. Guidelines for drinking-water quality. WHO Chron. 38, 104–108.
Wiemken, V., Theiler, R., Bachofen, R., 1981. Lateral organization of proteins in the chromatophore membrane of Rhodospirillum rubrum studied by chemical cross-linking. J. Bioenerg. Biomembr. 13, 181–194.
Witham, C.S., Oppenheimer, C., Horwell, C.J., 2005. Volcanic ash-leachates: a review and recommendations for sampling methods. J. Volcanol. Geoth. Res. 141, 299–326.